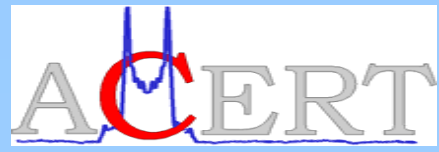

Electron Spin Resonance Spectroscopy: A Renaissance

Jack H. Freed
Department of Chemistry and Chemical Biology & ACERT
Cornell University
Ithaca, NY, USA

ACS 235th National Meeting
Physical Chemistry Awards Symposium
New Orleans, LA April 8, 2008

National Center for Research Resources
NATIONAL INSTITUTES OF HEALTH

A RENAISSANCE

In the 1960's both ESR & NMR were of comparable interest to physical chemists.

During the 1970's & 1980's NMR assumed its great prominence in chemistry, biology & physics that continues to this day.

In the last decade or so, new developments have led to a revitalization of ESR which parallels the earlier developments in NMR.

KEY DEVELOPMENTS & THEIR APPLICATIONS INCLUDE:

1. Very-High-Field & Frequency ESR: Quasi-Optical Methods.
2. Improved Modeling of Dynamic ESR Spectra: Stochastic Liouville Equation.
3. Two-Dimensional Fourier-Transform ESR: Intense Nano-second cm.- & mm.-wave coherent pulses.
4. Pulsed Dipolar ESR Spectroscopy & Protein Structure
5. ESR Microscopy

Molecular Dynamics by ESR

Introduction: What is special about ESR, in particular spin-label ESR? (e.g. compared to NMR)

1. ESR is much more sensitive per spin (than NMR).

2. In time domain experiments ESR's time-scale is nanoseconds (NMR's is milliseconds).

3. The spin-label spectrum is simple, & can focus on a limited number of spins.

4. ESR spectra change dramatically as the tumbling motion of the probe slows, thereby providing great sensitivity to local "fluidity".
   In NMR nearly complete averaging occurs, so only residual rotational effects are observed by T_1 & T_2.

5. Multi-frequency ESR permits one to take "fast-snapshots" using very high-frequencies & "slow-snapshots" using lower frequencies to help unravel the complex dynamics of bio-systems.

6. Pulsed ESR methods enable one to distinguish homogeneous broadening reporting on dynamics vs. inhomogeneous broadening reporting on local structure.

ESR Spectra in a Fluid

PDT/Toluene at 250GHz

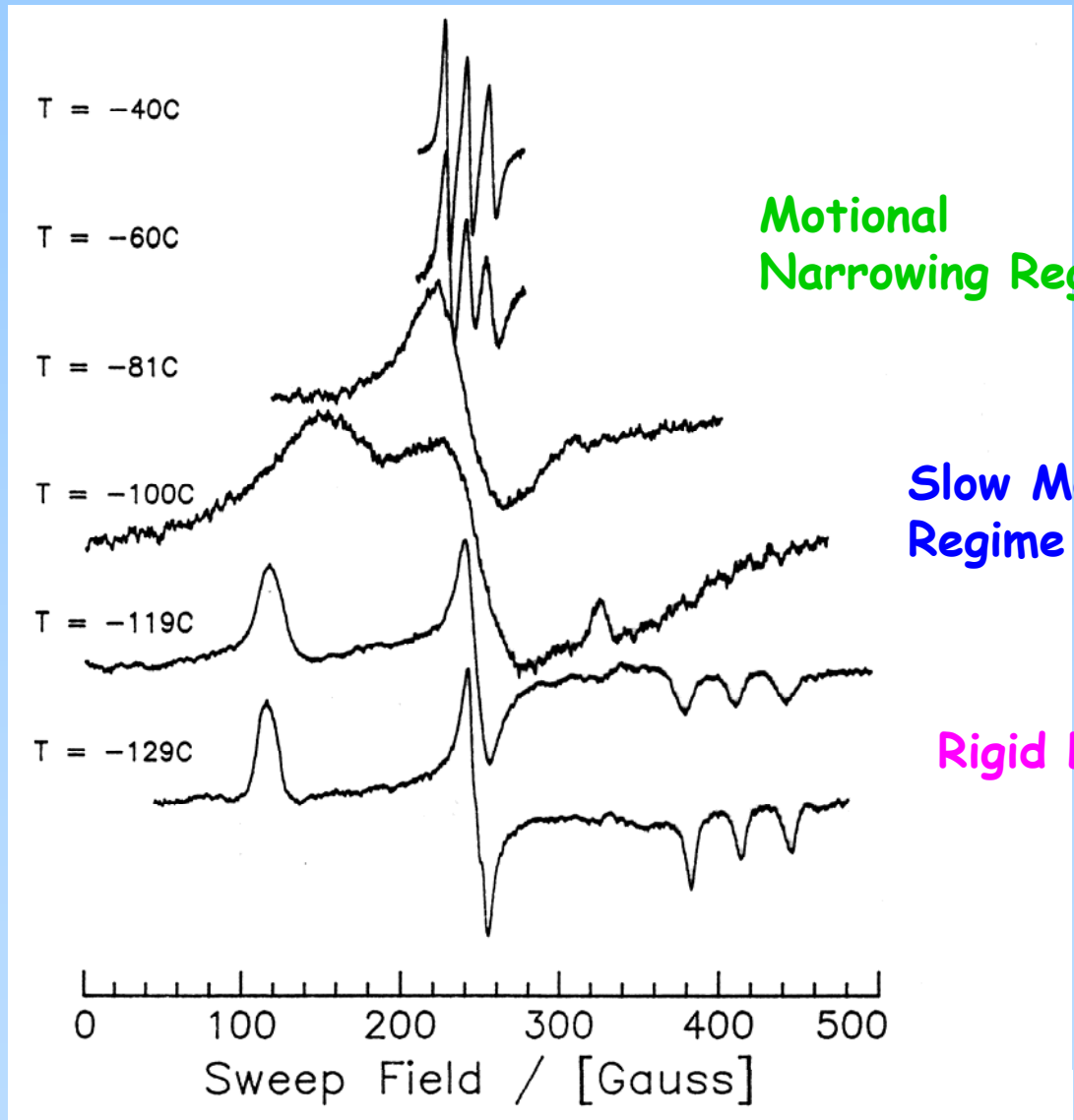

Motional Narrowing Regime

Slow Motional Regime

Rigid Limit

Multi-Frequency ESR Simulation

A motional process that looks fast at lower frequencies

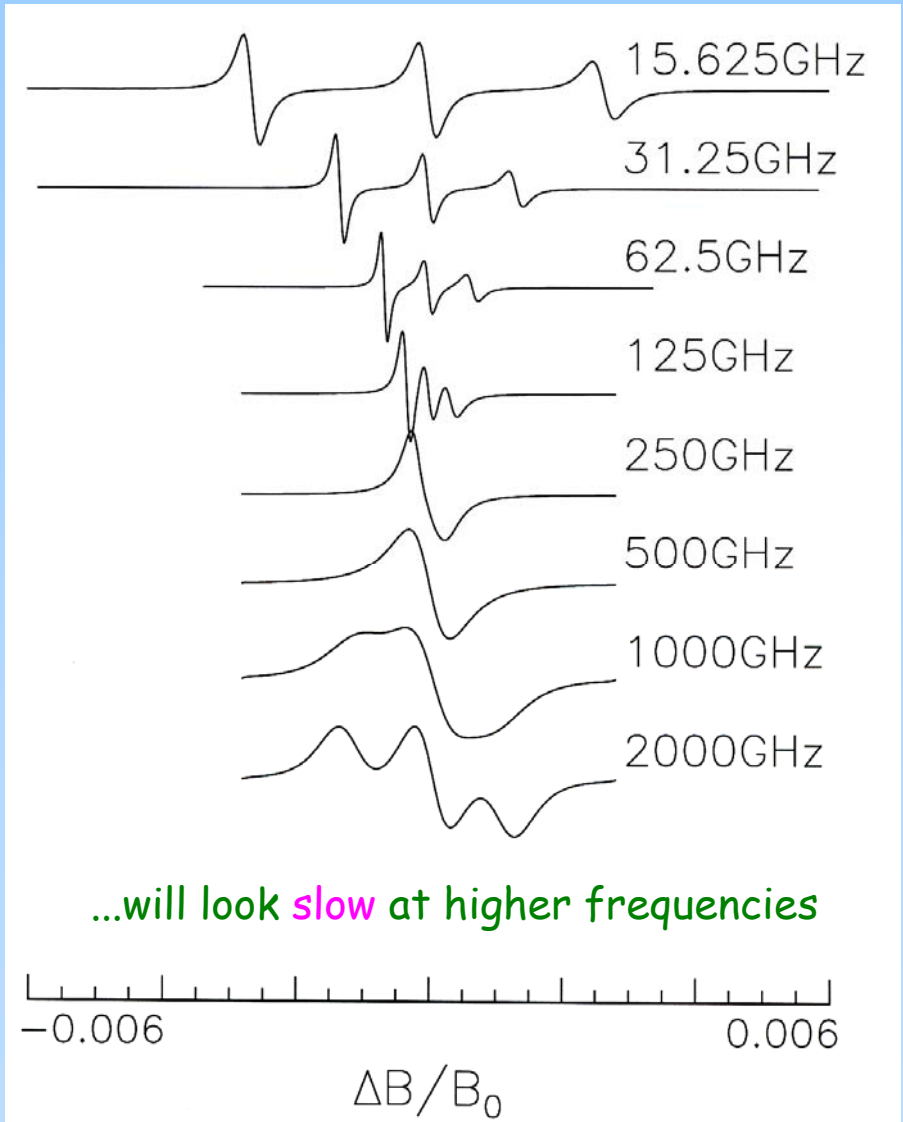

For complex dynamics of proteins

The slow overall & collective motions will show up best at lower frequencies

Whereas

The fast motions will show up best at higher frequencies

Rotational Tumbling Time:

$\tau_R = 1.7 \times 10^{-9}$ sec

ESR Spectra of aqueous solutions of T4 Lysozyme spin-labeled at mutant site 131 at different frequencies & temperatures *

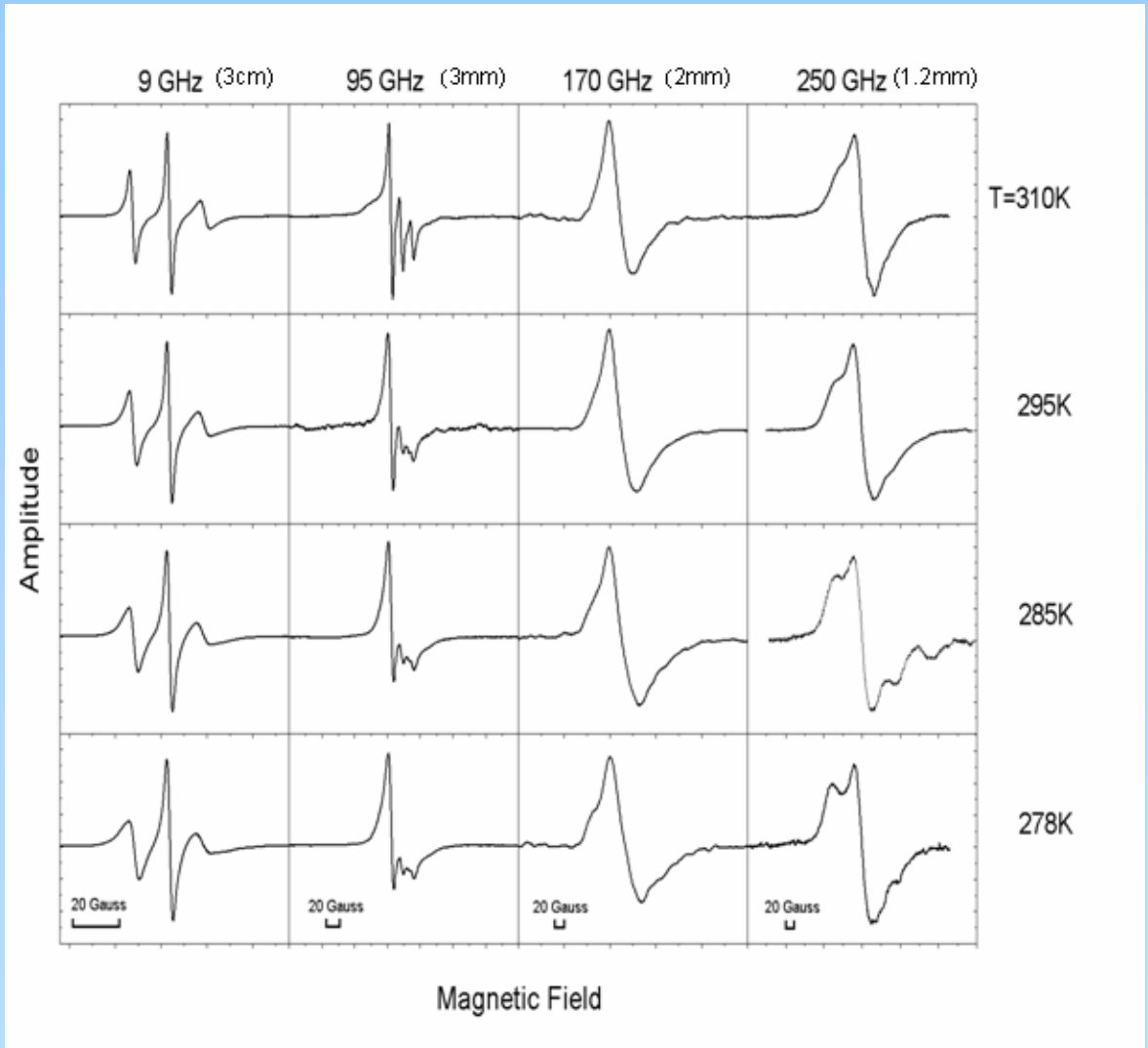

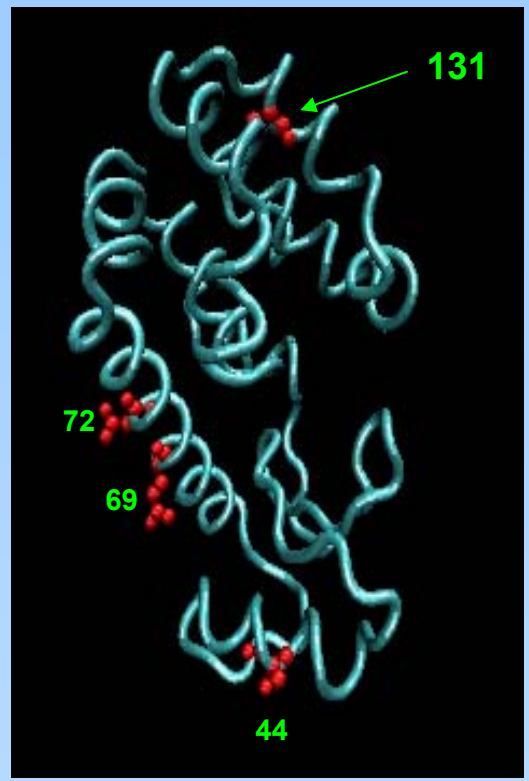

* V_s ~ 0.2µL

Sensitivity to Anisotropic Motional Dynamics: High Frequency

Example : complexes of cyclodextrins with spin-labeled fatty acids

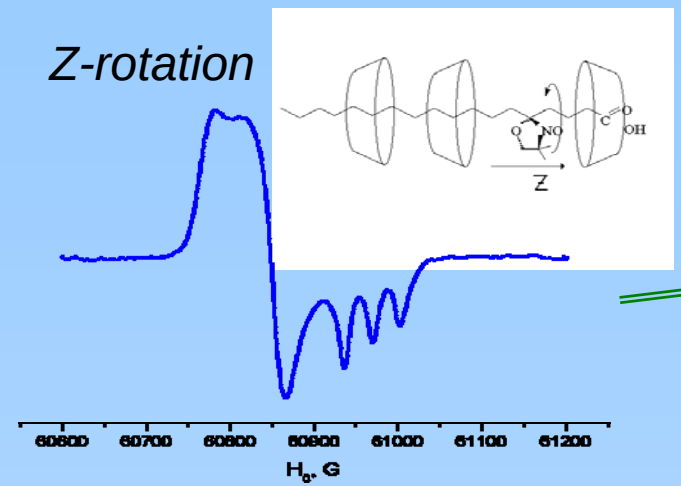

170 GHz

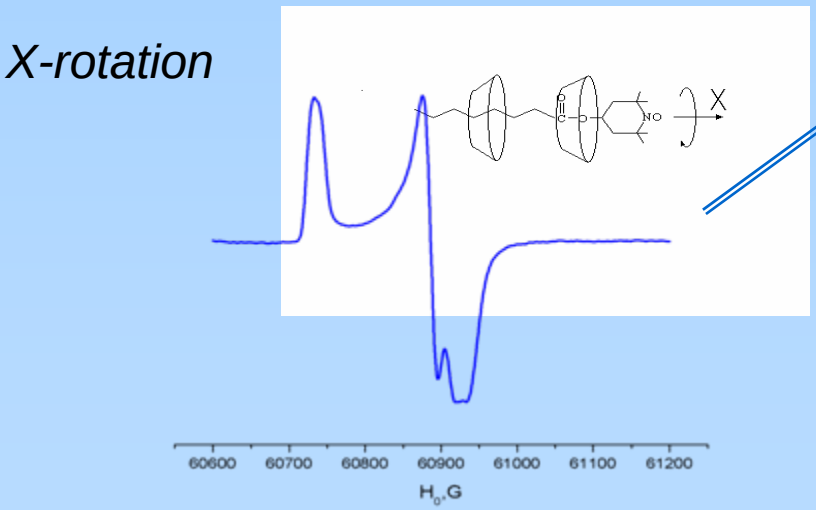

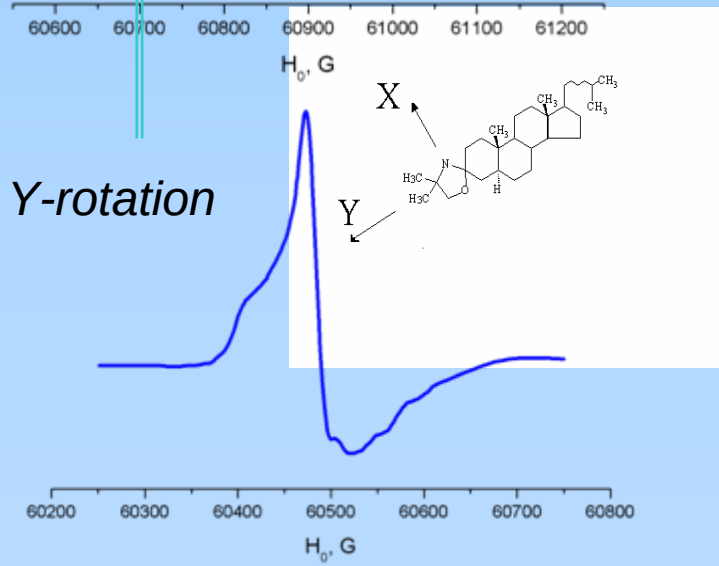

Schematic Diagrams of Quasi-Optical Bridges

Reflection Bridge →

Induction Bridge →

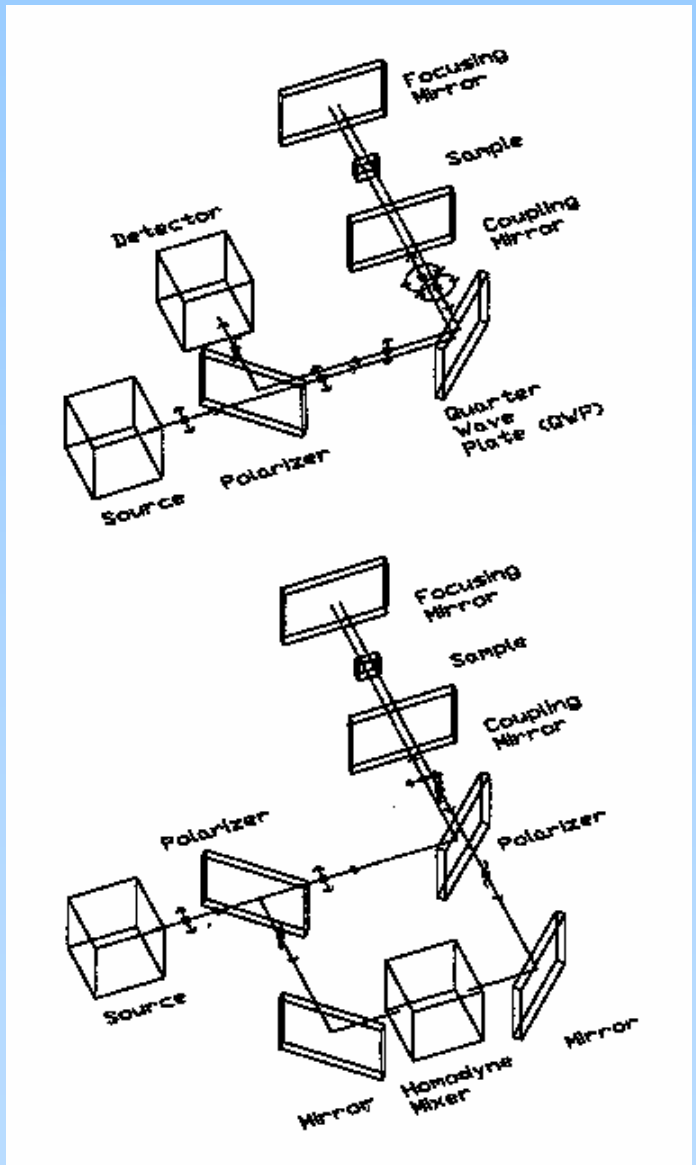

*From Appl. Magn. Res (1999)

Stochastic Liouville Equation

Assuming the "statistical independence" of the spin evolution & the molecular tumbling we may combine

the spin-density matrix, $\rho(t)$, and

the orientational distribution function, $P(\Omega,t)$ into

a combined spin and orientational distribution function, $\rho(\Omega,t)$, obeying:

$$\frac{\partial\rho(\Omega,t)}{\partial t} = -i\left[\hat{H},\rho\right] - \hat{\Gamma}_{\Omega}\rho(\Omega,t)$$

which is the stochastic Liouville equation (SLE).

- Note, that we recover the normal density matrix by averaging $\rho(\Omega,t)$ over all Ω :

$$\rho(t) = \left\langle \rho(\Omega,t) \right\rangle_{\Omega}$$

and we recover $P(\Omega,t)$

by setting the spin(s) S, I = 0.

The SRLS Model: A Mesoscopic View
e.g. A Spin-Labeled Protein

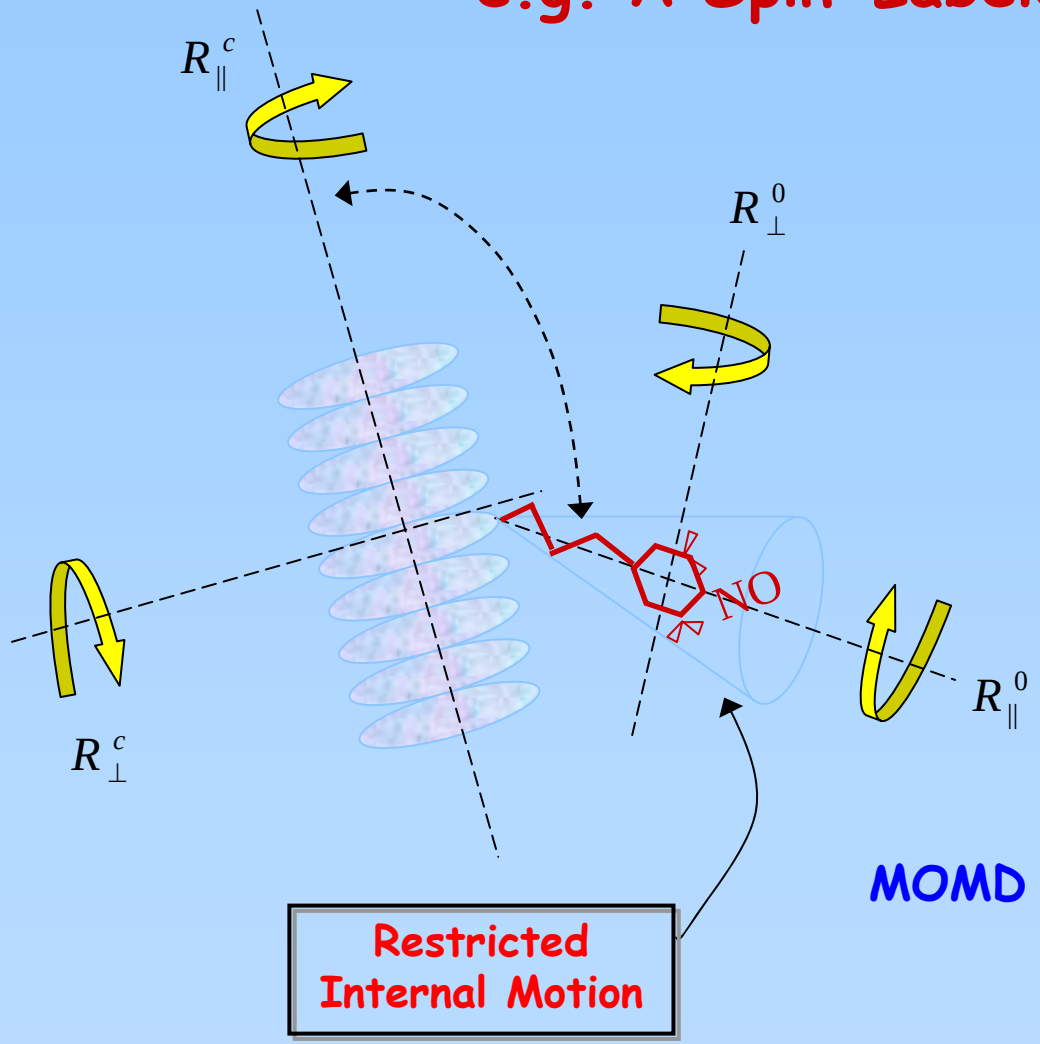

G-tensor frame

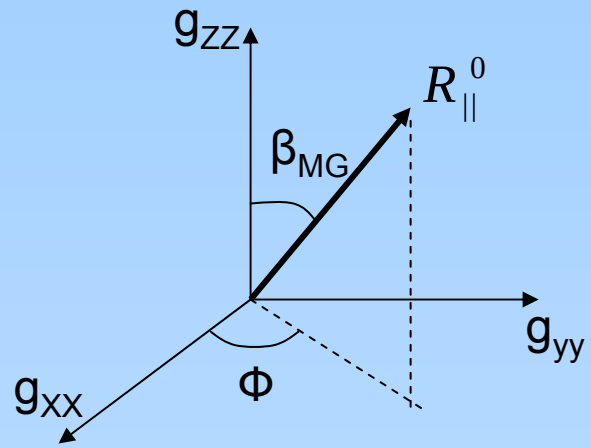

MOMD Model: $R_{\parallel}^{0}$ and $R_{\perp}^{c} \longrightarrow 0$

Multifrequency SRLS: T4 lysozyme

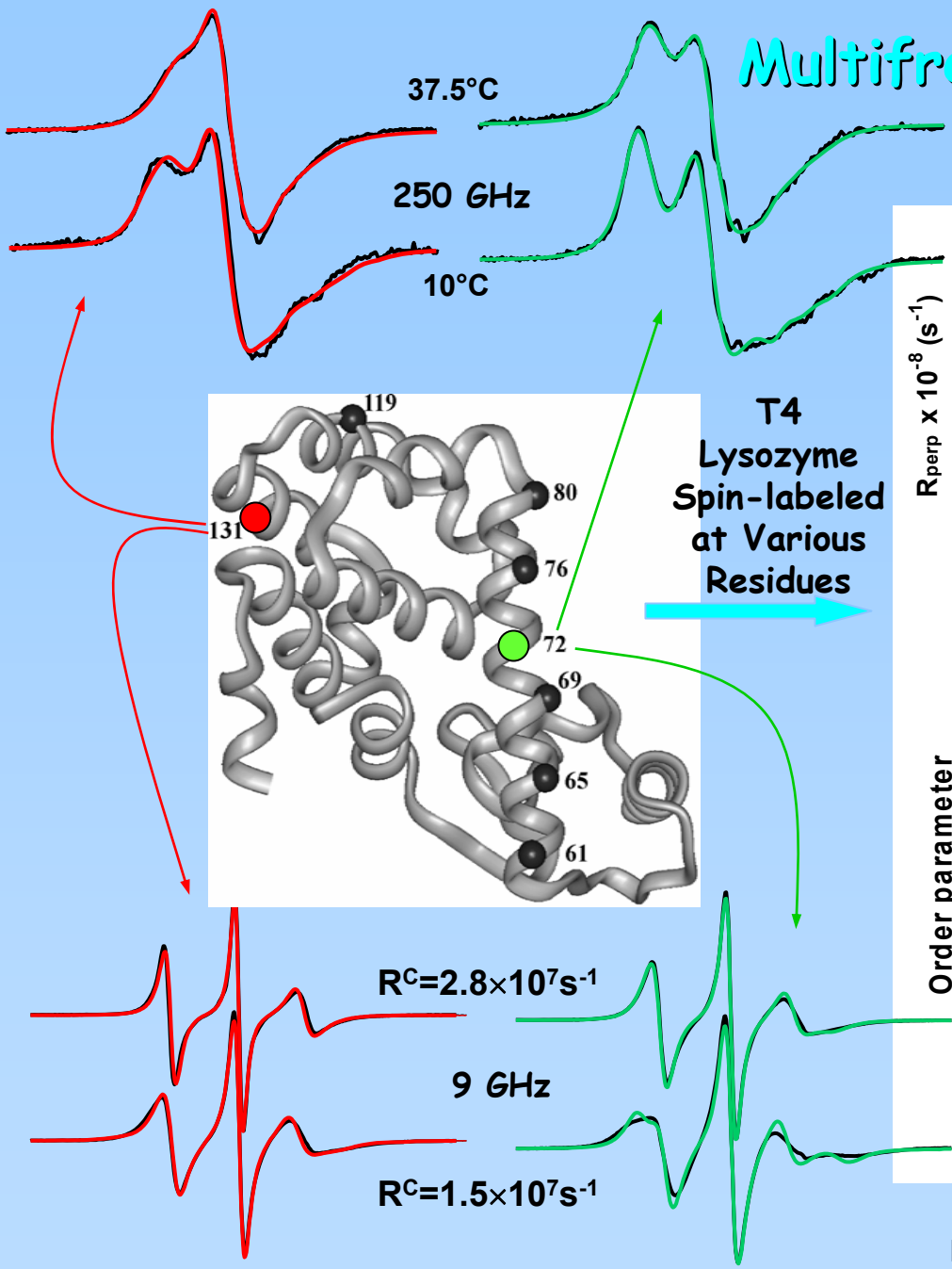

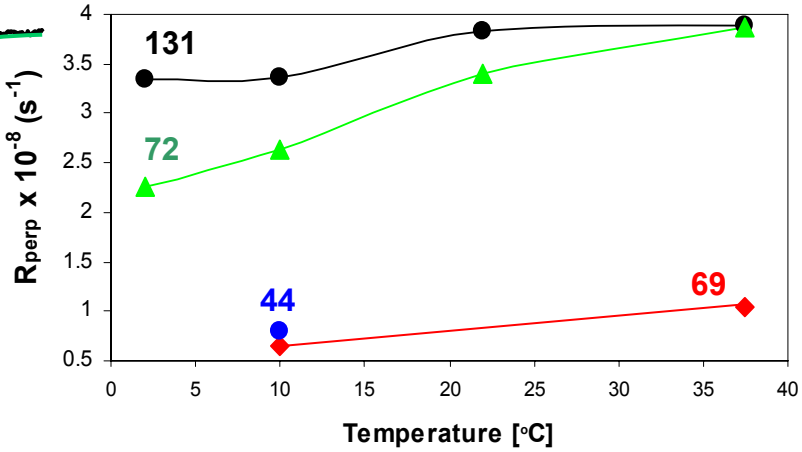

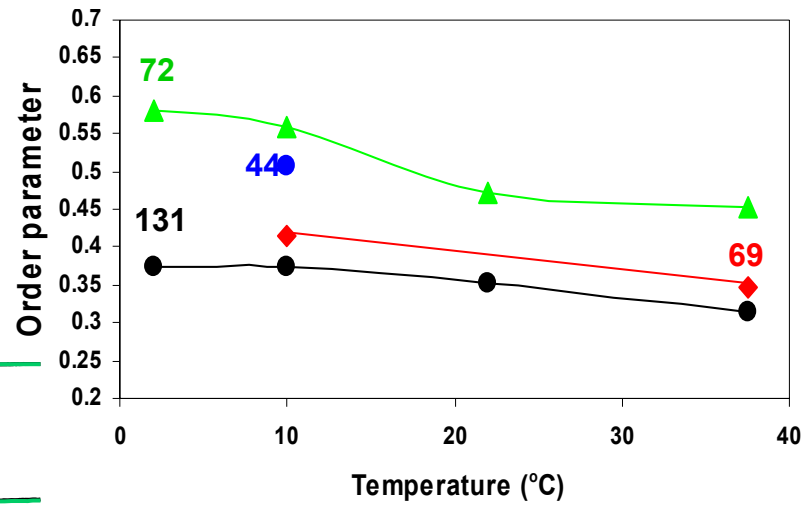

Liang *et al.* J. Phys. Chem. (2004) with W. Hubbell

Protein Dynamics by ESR

- **Can use high-frequency** (e.g. 250 GHz) **to "freeze-out" overall tumbling motions**, (& other slow motions).
- **This provides dramatic sensitivity to the faster local motions**: local ordering, local diffusion tensor, geometry.
- **Multi-frequency approach allows separation of different dynamic modes**.
- **Site-directed spin labeling is efficient**. Can produce about 10 mutants in one week.
- **Must account for motions of spin label tether, which however is restricted, & newer spin labels further restrict them.**

Molecular Dynamics Simulations: An Atomistic View *

Spin label dynamics

Experimental ESR spectrum

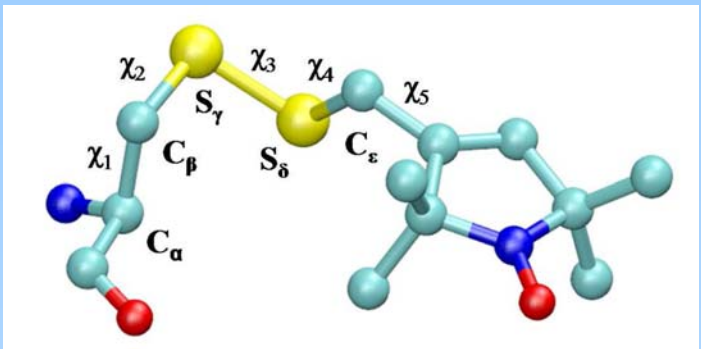

R1 Side-Chain containing nitroxide moiety

Protein X-ray structure

$$\hat{H}(t) = \gamma_e \left(\boldsymbol{B} \cdot \mathrm{G}(t) \cdot \hat{\boldsymbol{S}} + \hat{\boldsymbol{I}} \cdot \mathrm{A}(t) \cdot \hat{\boldsymbol{S}} \right)$$

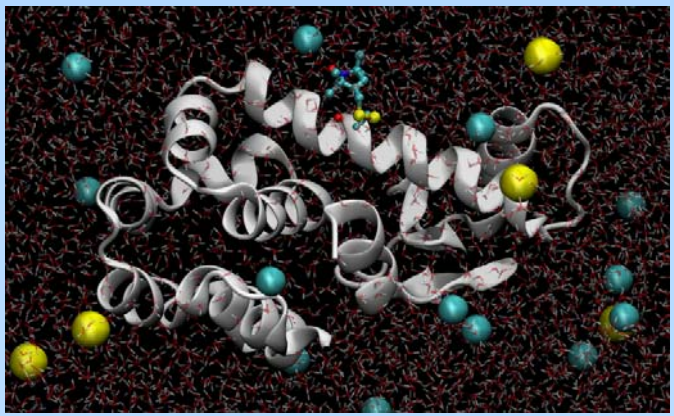

time domain

Calculated ESR spectrum

Atomistic MD simulations

* D. Sezer, J. H. Freed & B. Roux

Fits to Multi-frequency Spectra

——— experiment*

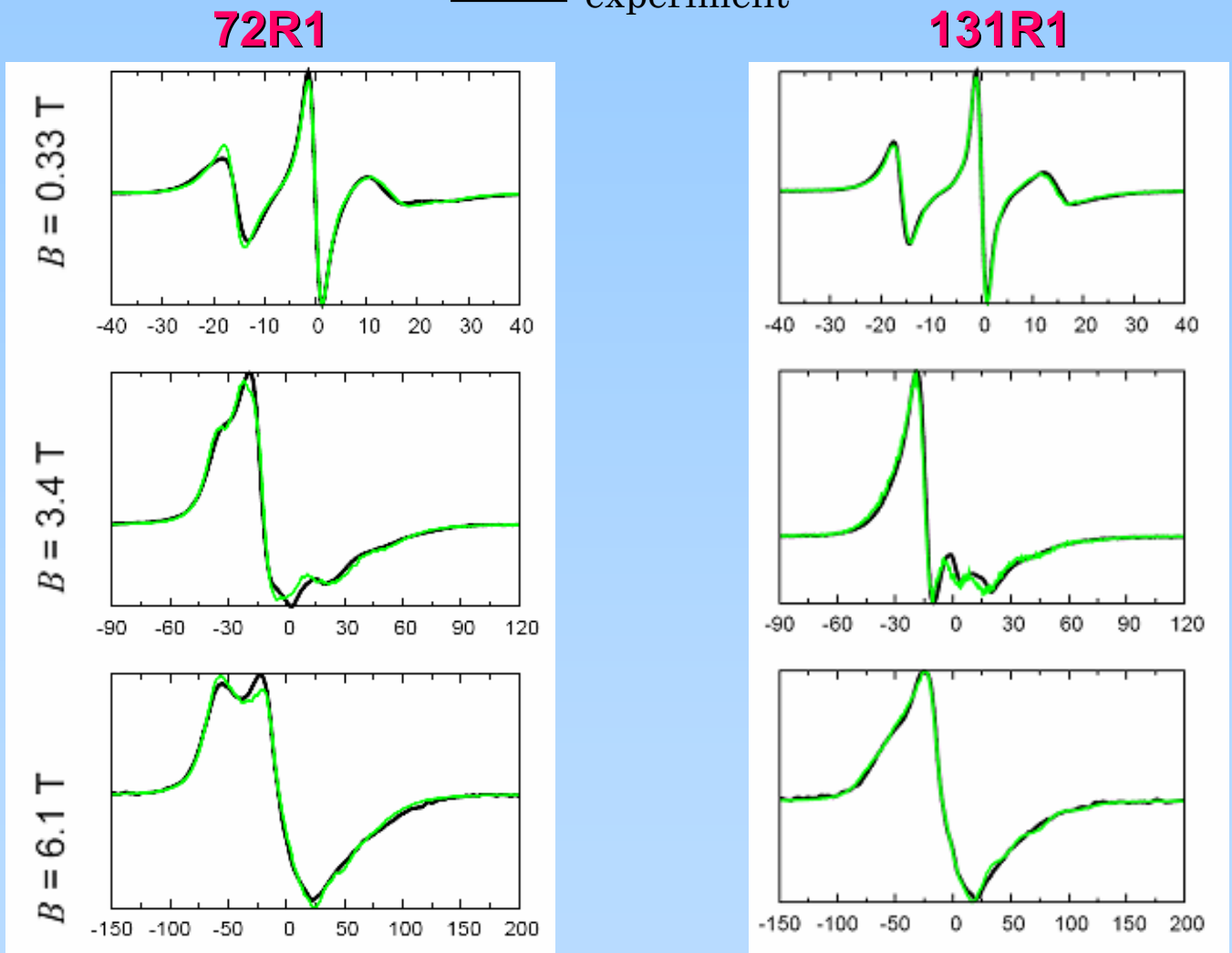

Comparison of 72R1 and 131R1

72R1

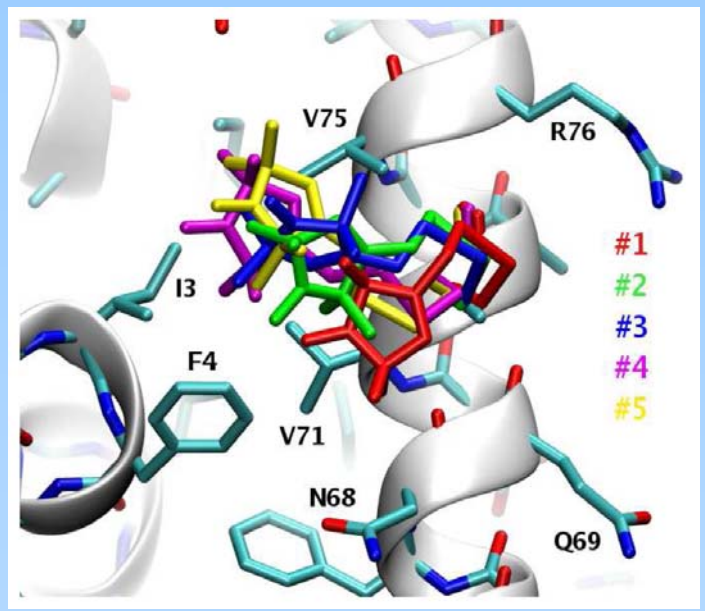

131R1

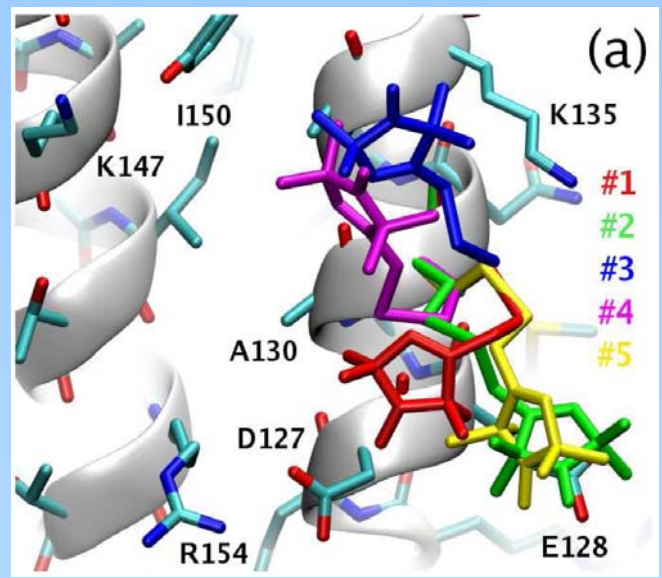

Conformations of the five most populated Markov states for 72R1 and 131R1.

Summary: MD and ESR

1. Exact time-domain integrators were required for the quantal dynamics of the spins and for the classical motions of the protein.

2. Force field parameters were needed for the side chain R1.

3. A systematic procedure for estimating a Markov chain model of the internal R1 dynamics from its MD trajectories was necessary to deal with the longer time scales needed.

4. The formalism was successfully applied to R1 at solvent-exposed sites in T4 Lysozyme.

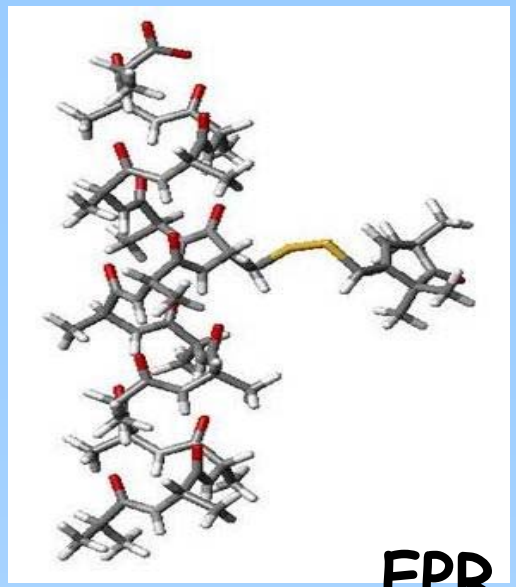

Adding Atomistic Perspective to Mesoscopic (SLE) Approach *

- model system: R1 linked to poly-Ala a-helix
- conformational analysis $\Rightarrow$ **stable conformers**

  $\Rightarrow$ **chain dynamics**

No Free Parameters

EPR spectra of R1 in α-helix domain

- overall protein reorientations
- side chain dynamics $\Leftarrow$ **Assumption: Conformers with low barriers exhibit fast exchange**

  Conformers with high barriers exhibit no exchange

modified SLE:

$$\frac{\partial \rho(\Omega_D,t)}{\partial t} = -i\,\overline{\boldsymbol{L}(\Omega_D)}\,\rho(\Omega_D,t) - \left[T_2^{-1}(\Omega_D) + \Gamma(\Omega_D)\right]\rho(\Omega_D,t)$$

$\overline{\mathbf{L}(\Omega_D)}$ Liouville superoperator with magnetic tensors partially averaged by chain dynamics

$\Gamma(\Omega_D)$ diffusion operator for overall protein tumbling

$T_2^{-1}(\Omega_D)$ linewidth contribution from chain dynamics (Redfield theory)

* F. Tombolato, A. Ferrarini, J.H. Freed

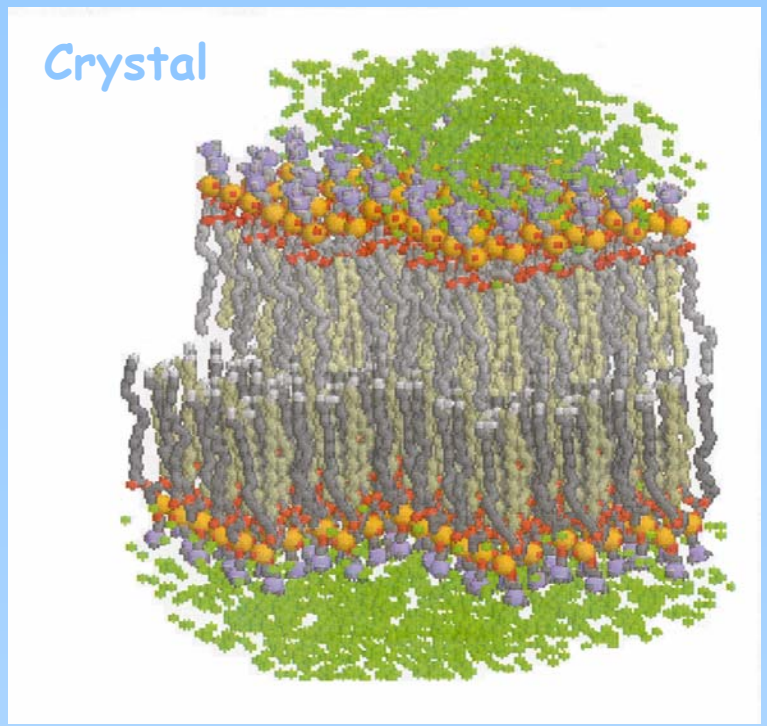

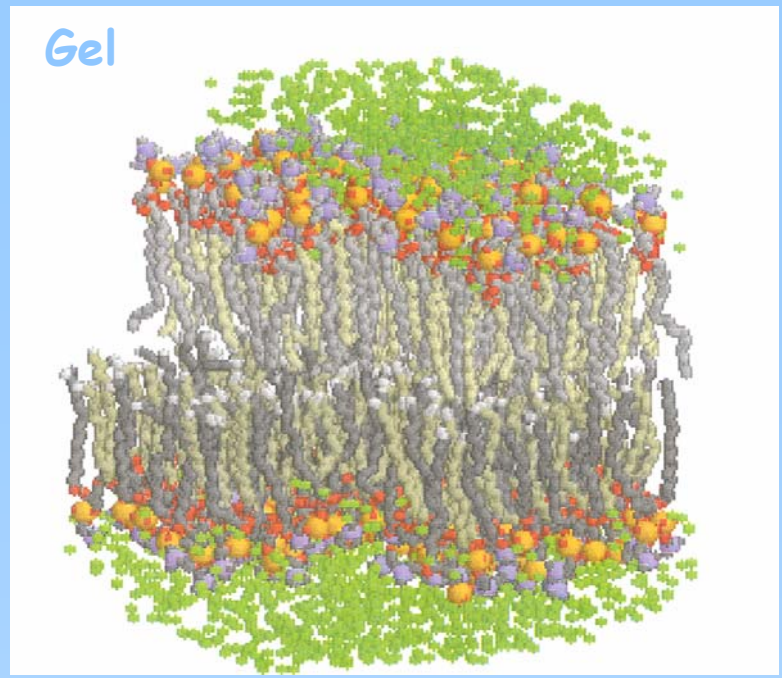

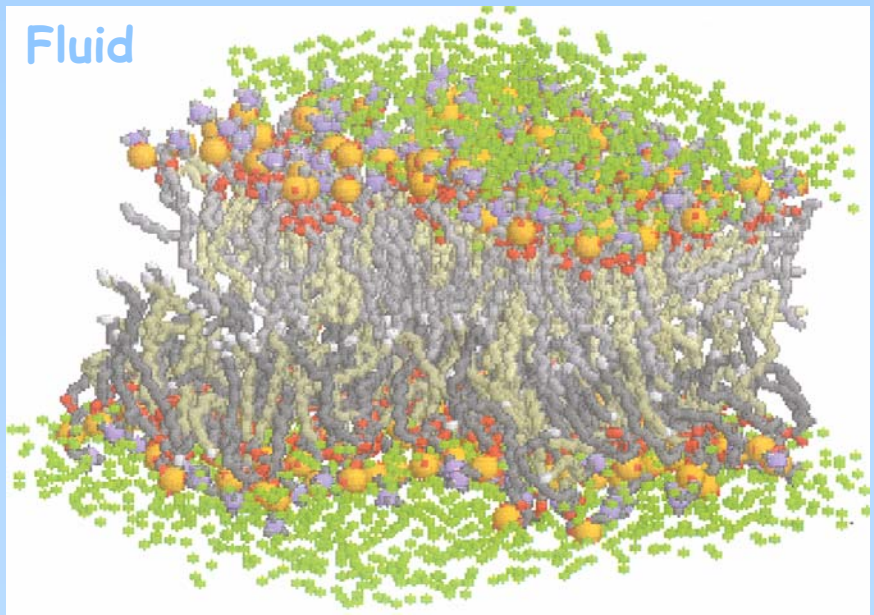

Molecular Dynamics Simulation of Phosphatidyl Choline (PC) Bilayer

Carbon/Palmitic, Water, Nitrogen,
Oleic, Phosphorus, Oxygen

Taken from: *H Heller, M Schaefer, K Schulten,J Phys Chem, 97:8343,1993, Rasmol Image by E Martz*

ESR on Live Cells

- ***Do rafts exist in plasma membranes?*** **It has been proposed that small rafts of Liquid-Ordered lipids exist in a "sea" of Liquid-Disordered lipids. ESR provides insight.**

- **How does the "dynamic structure" of *cell membranes* compare with that of *model membranes?***

CW-ESR Results from the Plasma Membranes of Four Cell Lines Showing Ordering (S_o) and Rotational Diffusion Rate ($R_\perp$) as a Function of Spin Label Position on the Acyl Chain. Two Components are Found in All Cases: a liquid-ordered (L_o) and a liquid-disordered (L_d). The fraction of the L_d spectral component is shown as $P(L_d)$.

Cell Line

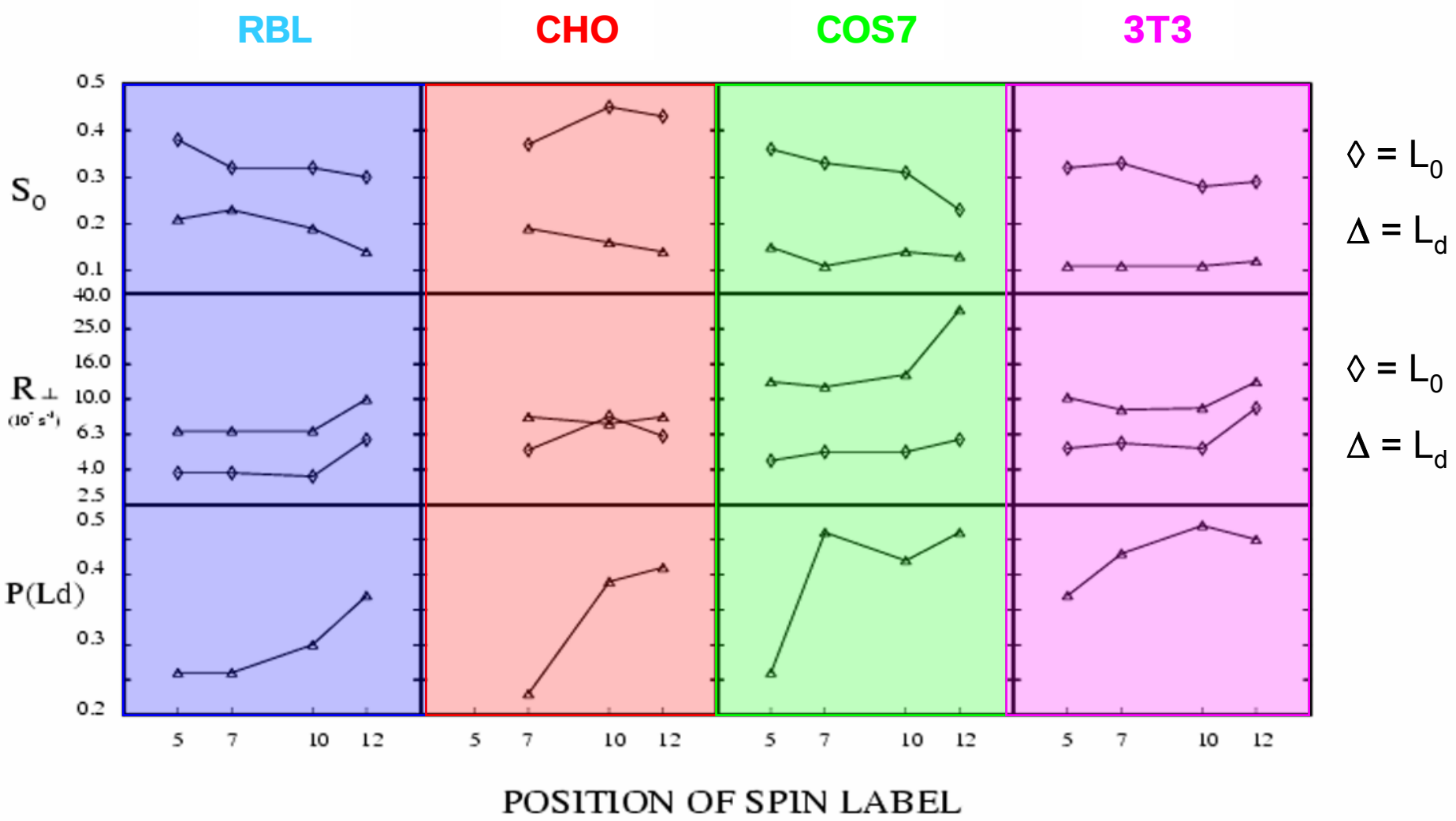

Comparison of Ordering (S_o) and Rotational Diffusion Rate ($R_\perp$) between SPM/DOPC/Cholesterol Model Membranes & Results for RBL/2H3 Cells

- - - - - = RBL/2H3 cell membrane

——— = model membrane

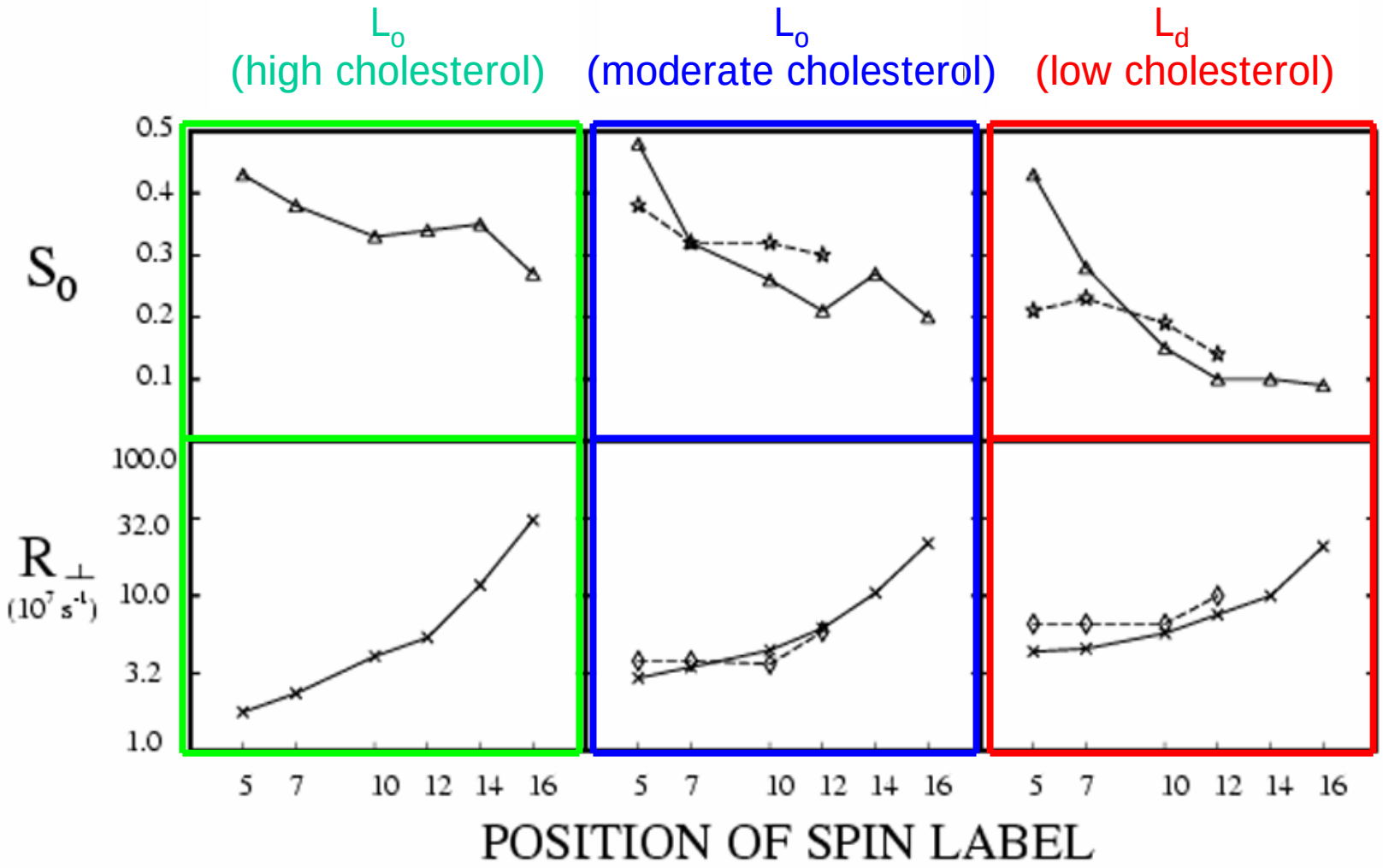

While such studies show the capabilities of cw-ESR for membrane studies, what is needed is an *improved ESR method* that:

1. More *readily* and *unambiguously distinguishes* the spectra from the different *components*, such as liquid-ordered (L_o) and liquid-disordered (L_d).

2. Enables a *more accurate assignment* of *dynamic* (i.e. $R_\perp$) and *ordering* (i.e. S_o) *parameters* to the separate spectral *components*.

Two-Dimensional Spectroscopy *

1976 - Richard Ernst, ETH: NMR: 300 cm (MDA)‡

1986 - Jack Freed, Cornell U.: ESR: 3 cm (MDA) ‡

2004 - ESR: 3mm

2000 - Robin Hochstrasser, U Penn: Vibrational Spectra: 6 μm (EDA) ‡

2005 - Graham Fleming, UC Berkeley: Optical Spectra: 0.8 μm (EDA) ‡

*** "Spectroscopy at a stretch," R. M. Hochstrasser, Nature, 434, 570 (2005).**

‡ MDA = Magnetic Dipole Allowed; EDA = Electric Dipole Allowed.

2D-ELDOR, A Powerful tool for Studying Membrane Dynamics Over Wide Temperature and Composition Ranges

Phases of Two Component System: DPPC/Chol

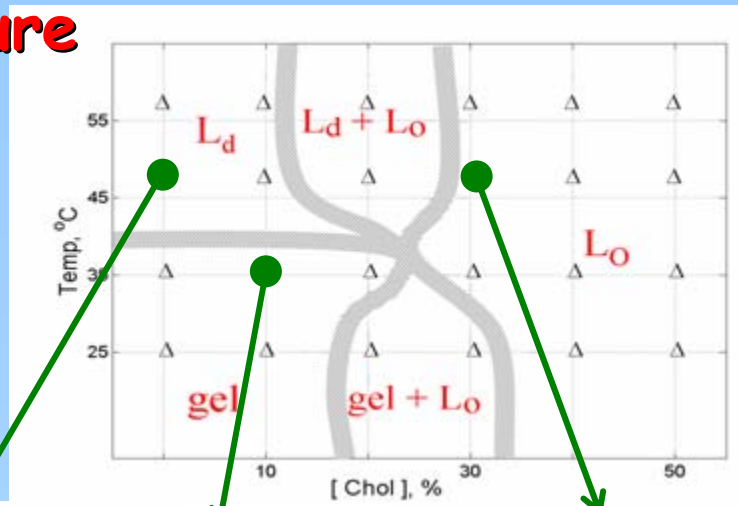

- The **spectra from an end-chain labeled lipid are distinctly different** in the three different phases.
- The **new** DPPC/Chol phase diagram determined by 2D-ELDOR is, in general, consistent with what was previously found.
- The **ordering and dynamics** are reliably obtained from the analysis of the 2D-ELDOR spectra.

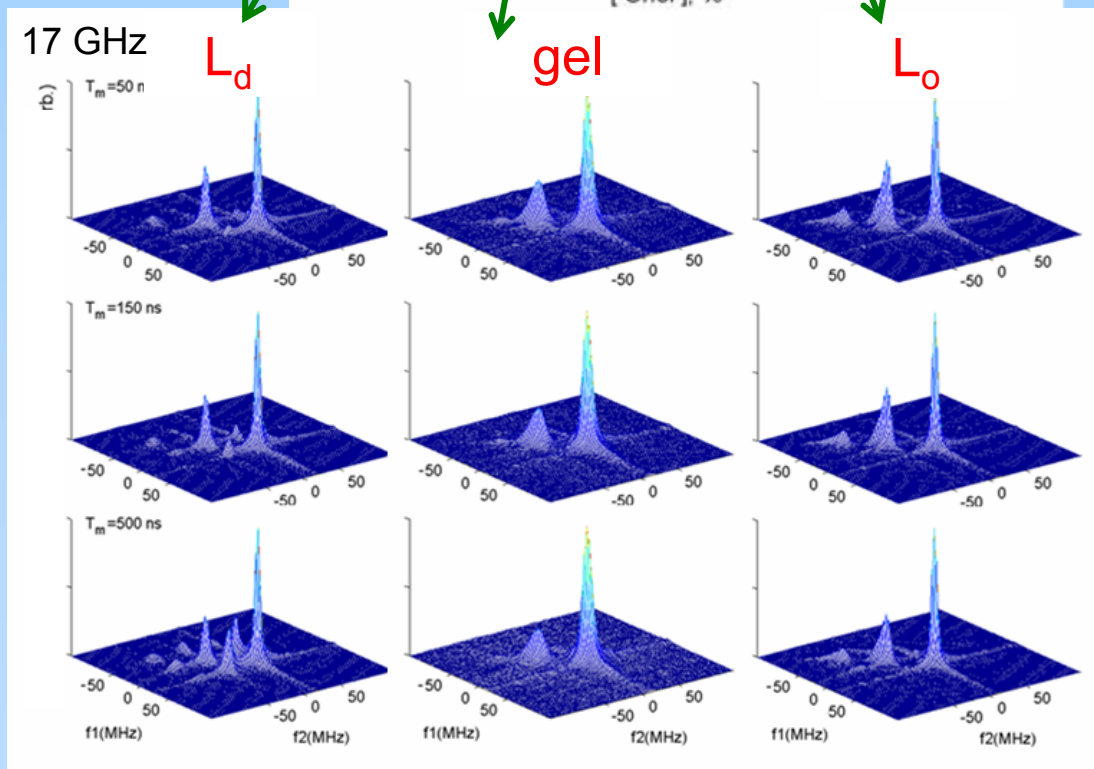

Initial 2D-ELDOR Studies Show Phase Structure Changes in Plasma Membrane Vesicles (PMV) from RBL Cells upon Stimulation

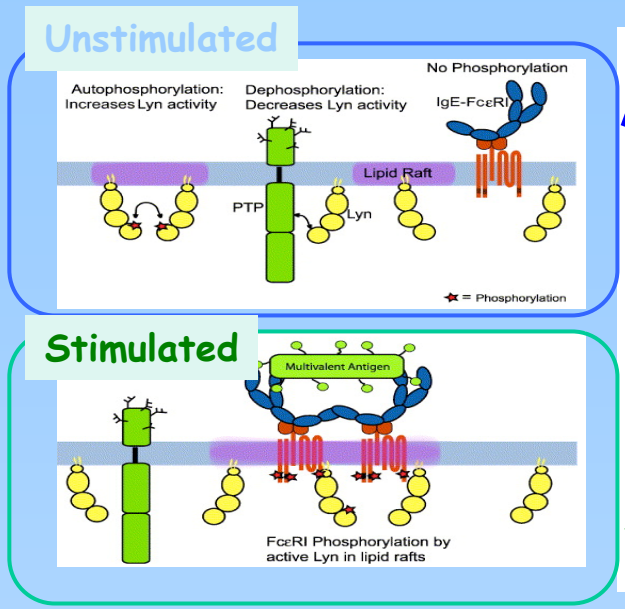

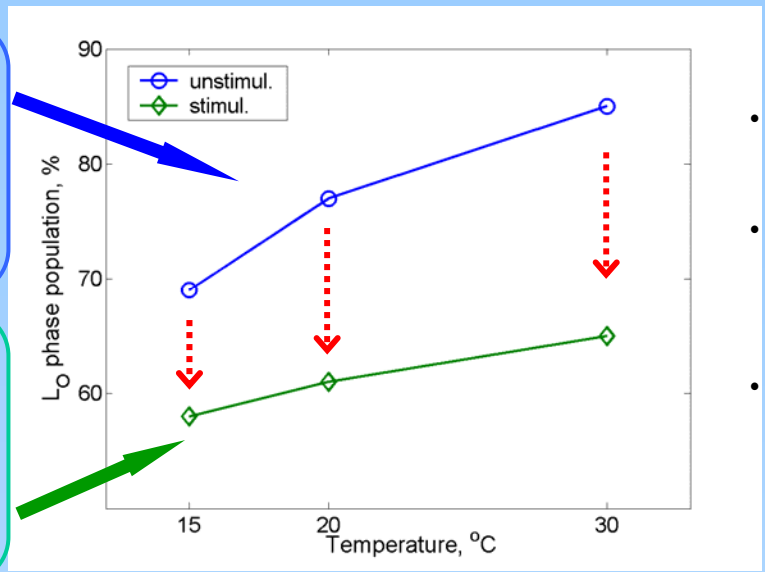

- 2-phase coexistence in PMV
- The population of the Lo phase decreases upon stimulation.
- The dynamic structure is revealed

2D-ELDOR provides better understanding of membrane phase structure in PMV.

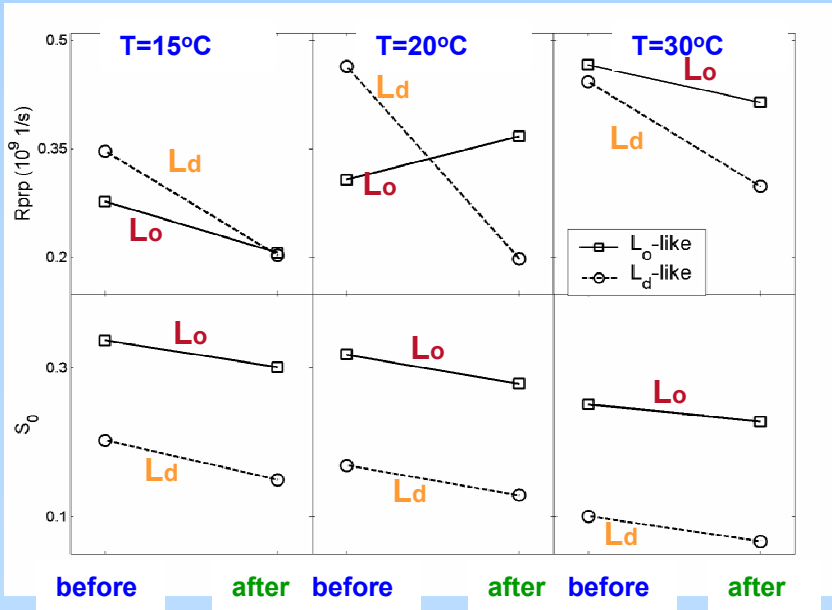

95 GHz Quasi-Optical High-Power Pulse Spectrometer

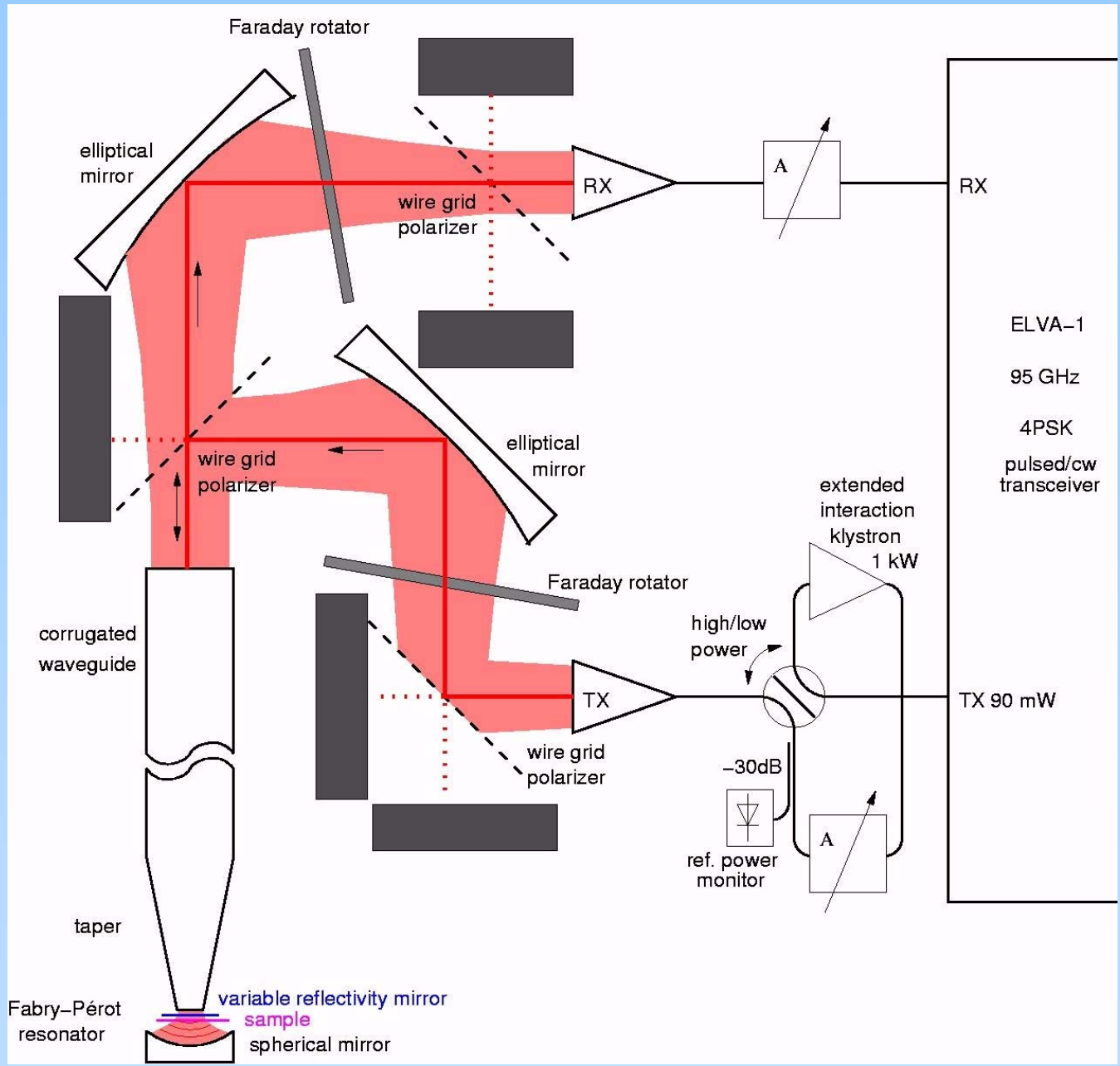

Oriented CSL/DPPC membranes at 17° C

cw-95 GHz

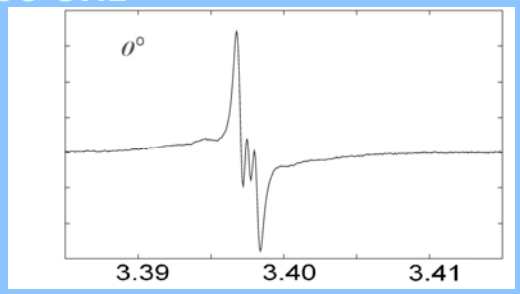

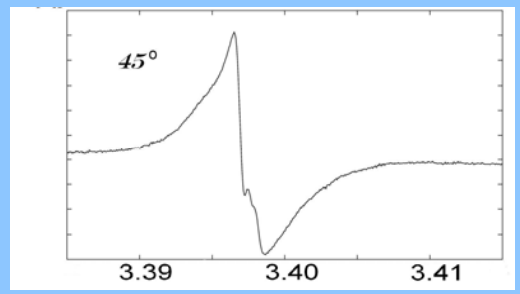

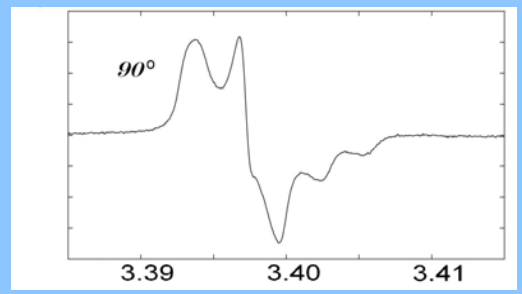

B_o[T]

95 GHz - *2D-ELDOR*, $\boldsymbol{B}_0 \| \hat{n}$

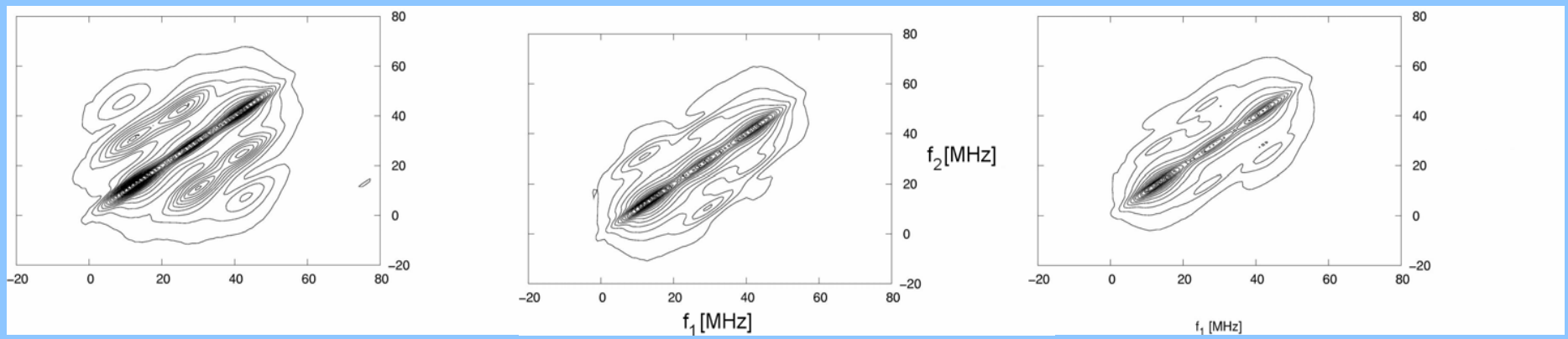

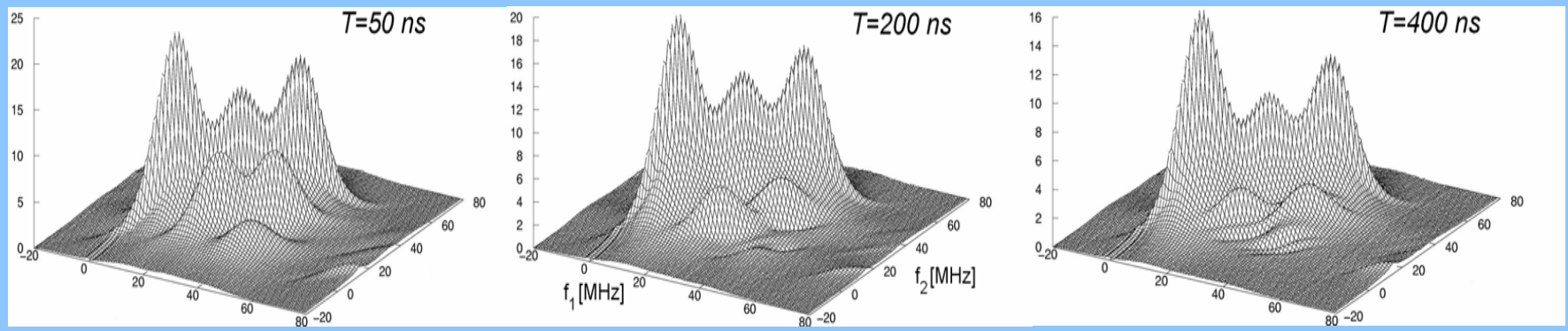

Pulse Dipolar ESR Spectroscopy & Protein Structure

- Many biological objects can be studied: soluble and membrane proteins and protein complexes, RNA, DNA, peptides, polymers.

- A variety of sample types possible: solutions, liposomes, micelles, bicelles, multi-bilayer vesicles, biological membranes.

- A variety of sample morphologies possible: uniform, ordered, heterogeneous, etc.

- Broad range of concentrations from micromolar to tens of millimolar is amenable. Only ca. 10 microliters of sample needed.

PDS ESR and Protein Structure

- Distances yielded by PDS span wide range of 10-80 Å and they are fairly accurate. Therefore, a relatively small number of them is sufficient to reveal structures. A single distance can address important structural and functional details.

- Several methods for data analysis greatly simplify the task of extracting average distances and distance distributions.

A "Zoo" of Proteins Studied at ACERT

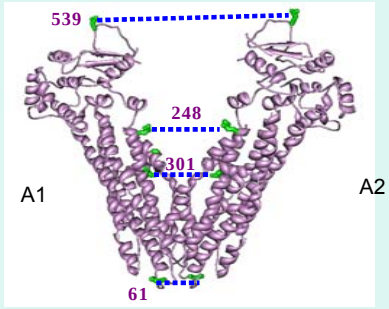

A1

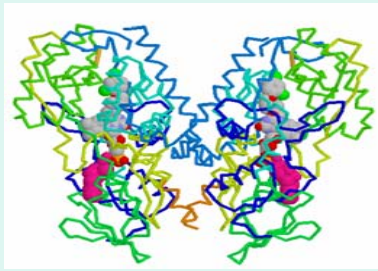

A2

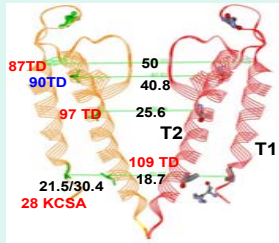

A3

B1

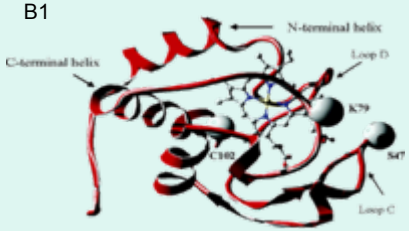

B2

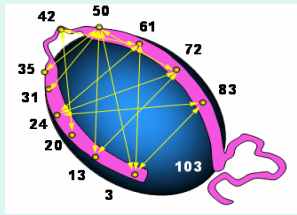

B3

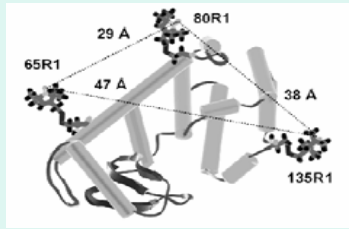

C1

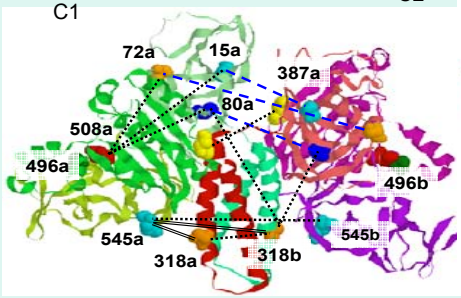

C2

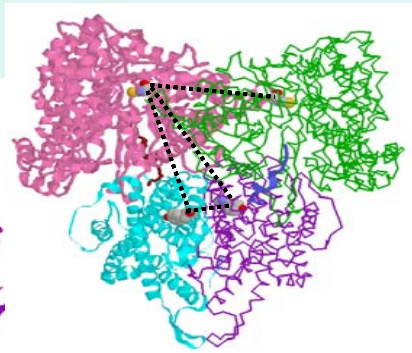

C3

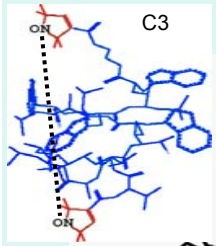

C4

DEER and DQC Pulse Sequences

DEER 4-pulse Sequence

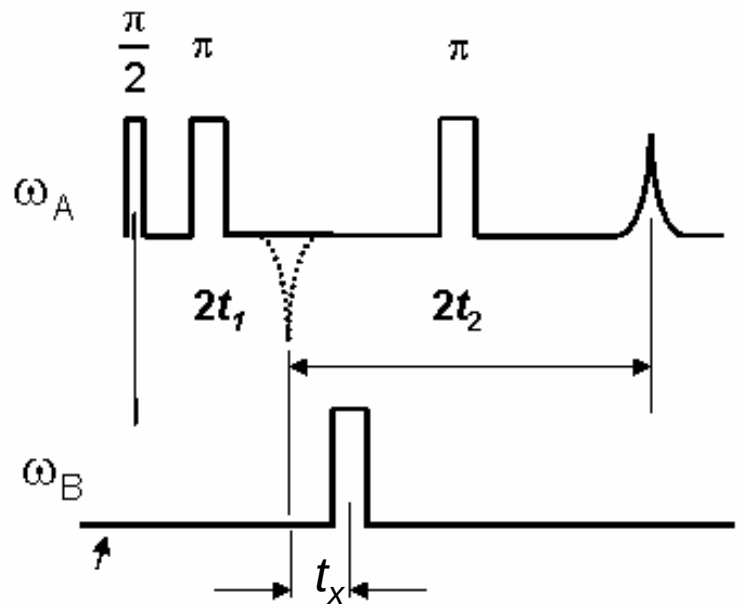

Signal amplitude $V = V_0[1 - p(1 - \cos \omega_d t_x)]$

Pump-probe technique irradiates only a fraction of spins with ca. 15-30 ns. pulses. (5-10G).

DQC 6-pulse Sequence

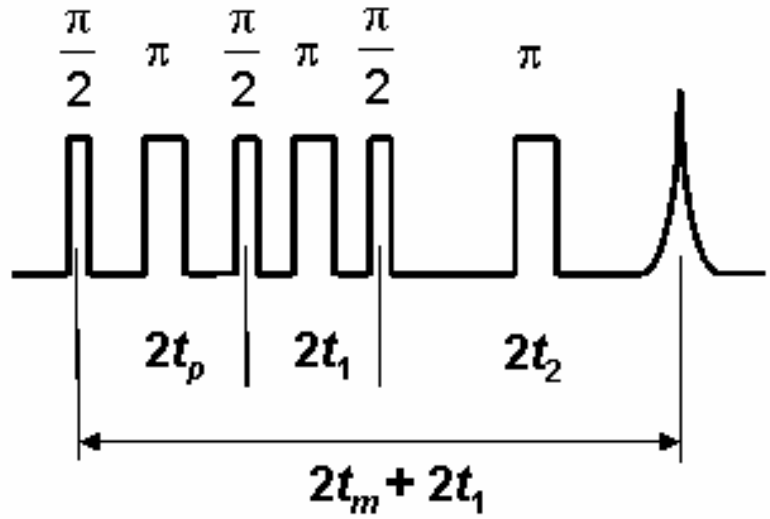

Signal amplitude

$$\omega_d = \frac{\gamma_e^2 \hbar}{r^3}$$

$$V = -\sin \omega_d t_p \sin \omega_d (t_m - t_p) = \frac{1}{2}[\cos \omega_d t_m - \cos \omega_d t_\xi]$$

$$t_\xi = t_m - 2t_p$$

Irradiates (nearly) all the spins with 3 ns. pulses (30-60G).

Signal Transduction in Chemotaxis

Bacteria swim to attractants and away from repellents by switching the sense of flagella rotation. A complex chain of events and multiple proteins and protein complexes are involved into the chemotactic response.

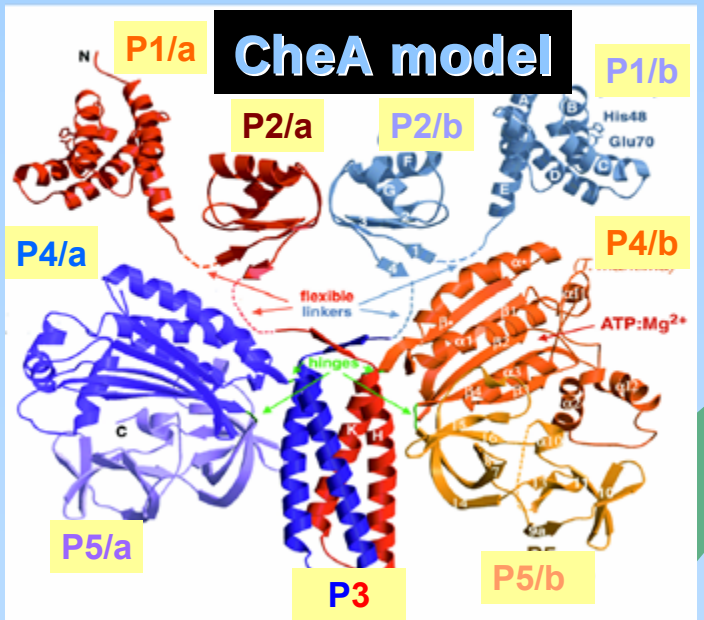

CheA is a homodimer assembled into 9 domains.

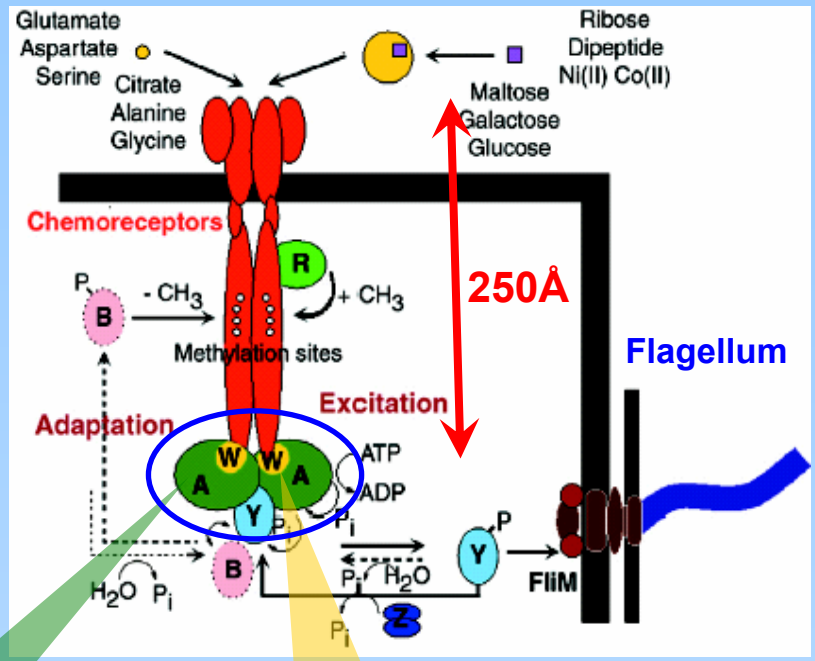

A bacterial chemoreceptor relays the signal over a 250Å distance to histidine kinase, CheA, where the phosphorylation cascade starts. CheA is attached to the receptor via the coupling protein, **CheW**.

Spin-labeling Sites and the Distances

A number of single and double cysteine mutants of CheAΔ289 were engineered for PDS study. CheA Δ289 complexes with labeled or unlabeled CheW in various combinations have been used.

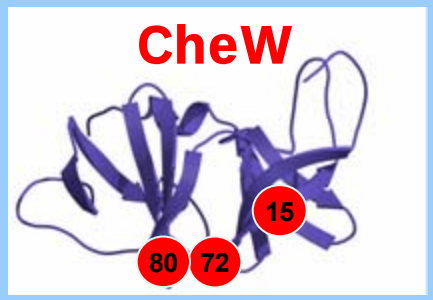

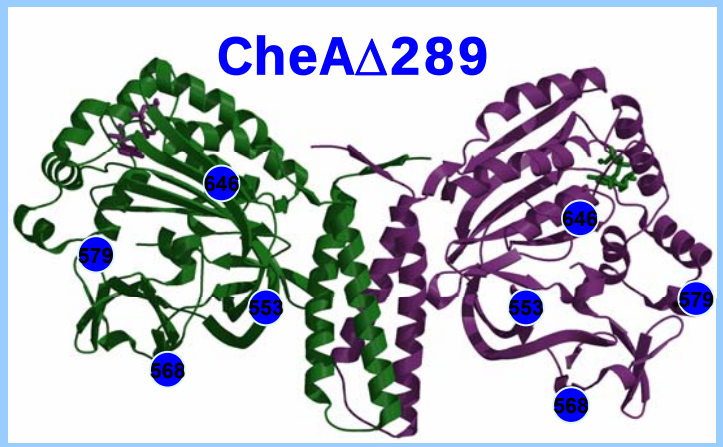

CheAΔ289 is a dimer and binds two **CheW**. Thus, there are **four electron spins**.

This complication was overcome by selecting spin-labeling sites such as to make the distances of interest distinct from the rest.

Mutated Residues

CheAΔ289: N553, E646, S579, D568

CheW: S15, S80, S72

Intra-domain and inter-domain distances, Å.

Mutated site	15	72	80	553	568	579	646
15		27&29	18.2	37	54.5	61	43.7
72	X		24.5&30	27	49	46	32.5
80	X	X		26	47	54.5	39.5
553	X	X	X		23.5	34.5	32
568	X	X	X	X		32.5	35.5
579	X	X	X	X	X		28
646	X	X	X	X	X	X	

PDS: "Triangulation"

The cartoon illustrates the "triangulation" grid of PDS constraints obtained to solve binding CheA-Δ289 P5 domain (blue) and CheW (pink).

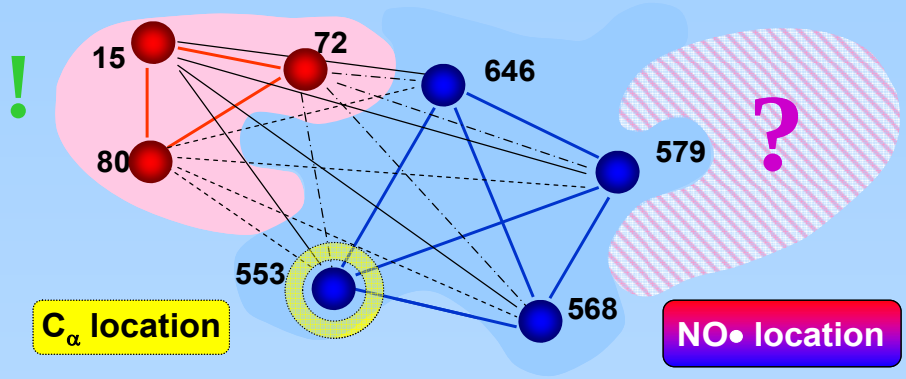

The spheres represent volumes occupied by the nitroxide groups. The increase in number of constraints (which are fairly accurate distances) reduces the uncertainty in the position of the backbone.

Example of Rigid Body Refinement by CNS*

Starting with random orientations of the two proteins, the program gives the final conformation of the P5/CheW complex.

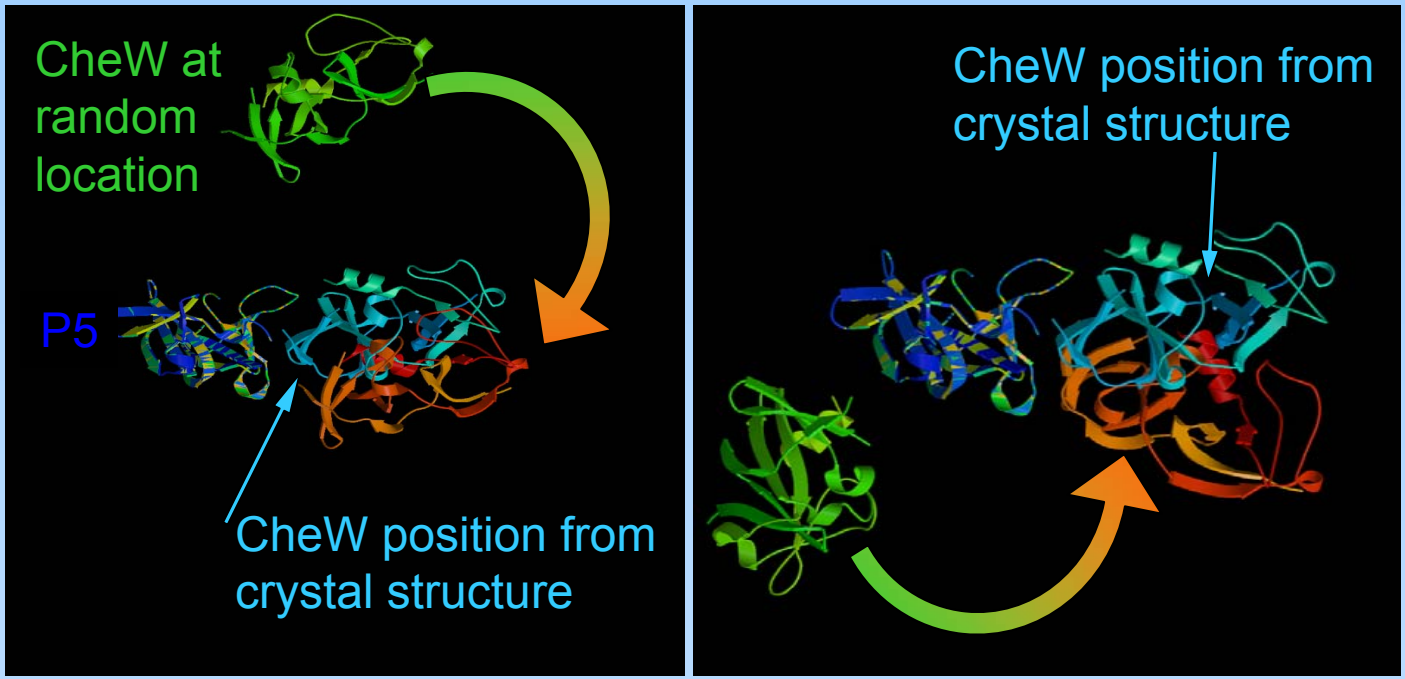

*CNS: Distance geometry software package for structure determination based on constraints from NMR or X-ray Crystallography.

Functional Dynamics of ABC Transporters (DEER)

Conformational Cycle of MsbA

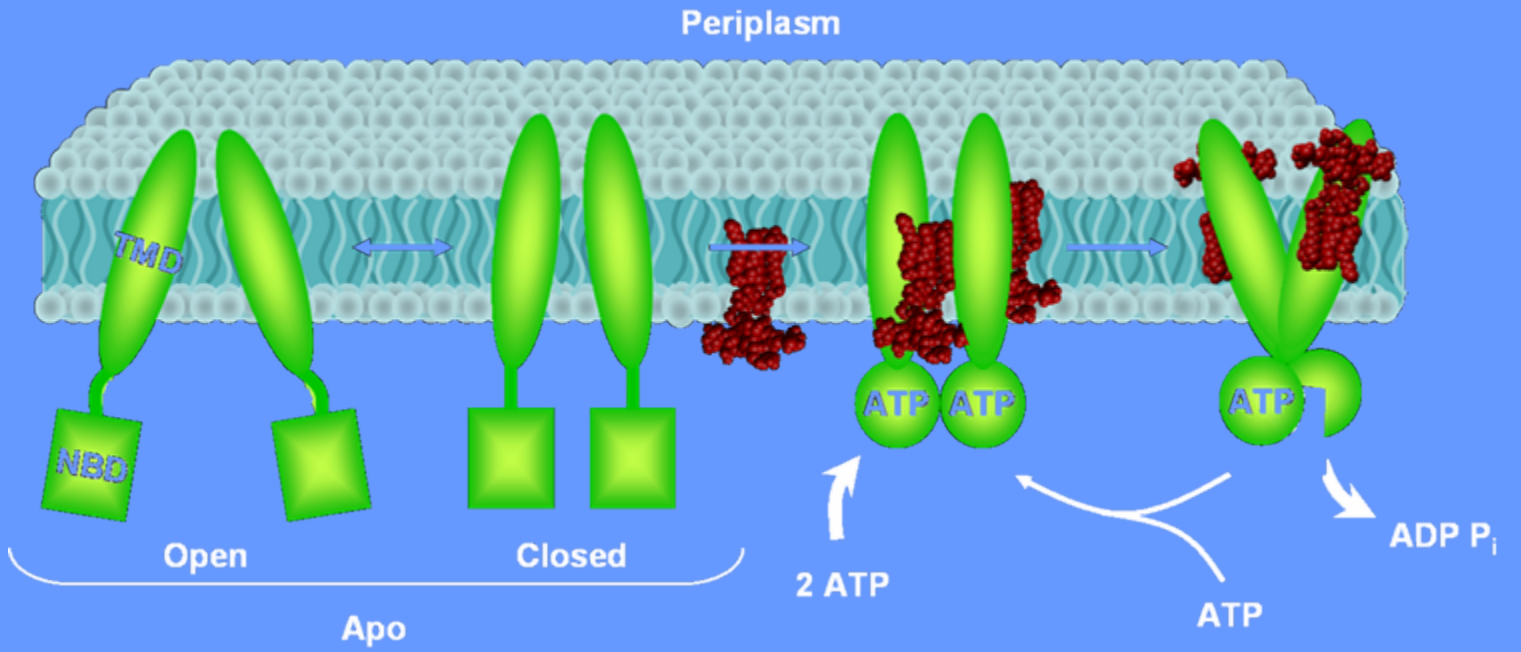

ABC transporters, such as MsbA, transport out of cells: cytotoxic drugs, structurally and chemically dissimilar molecules, against their concentration gradients. Energized by ATP hydrolysis, they act in a few power "strokes" culminating in drug expulsion.

The cartoon depicts flipping cytotoxic lipid (in brown) from the inner leaflet of the internal membrane of Gram-negative bacteria to the outer leaflet.

Dipolar Data and Distance Distributions for MsbA Reconstituted into Micelles & Liposomes

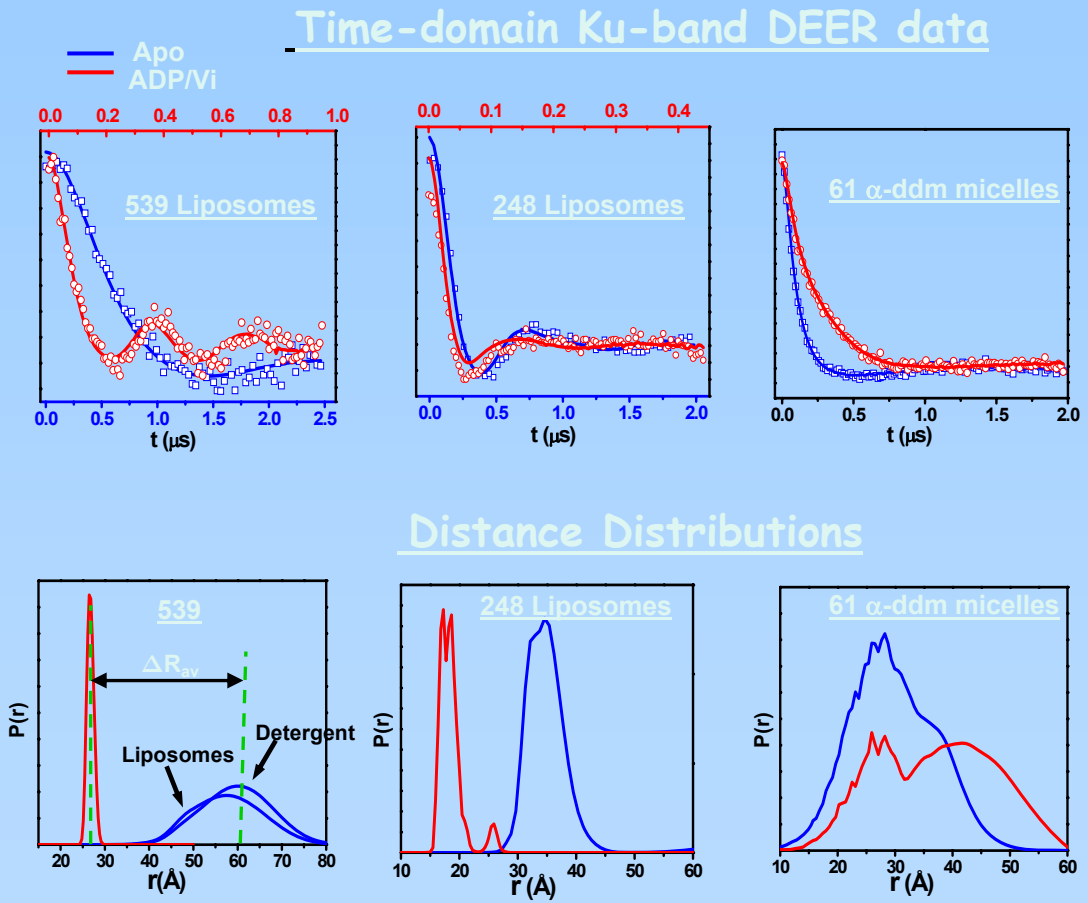

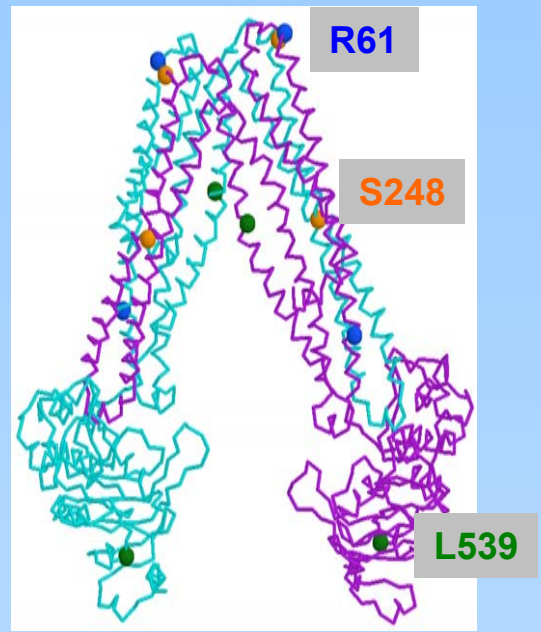

Reprocessed X-Ray Data Now Tells the Same Story as Pulsed and CW ESR

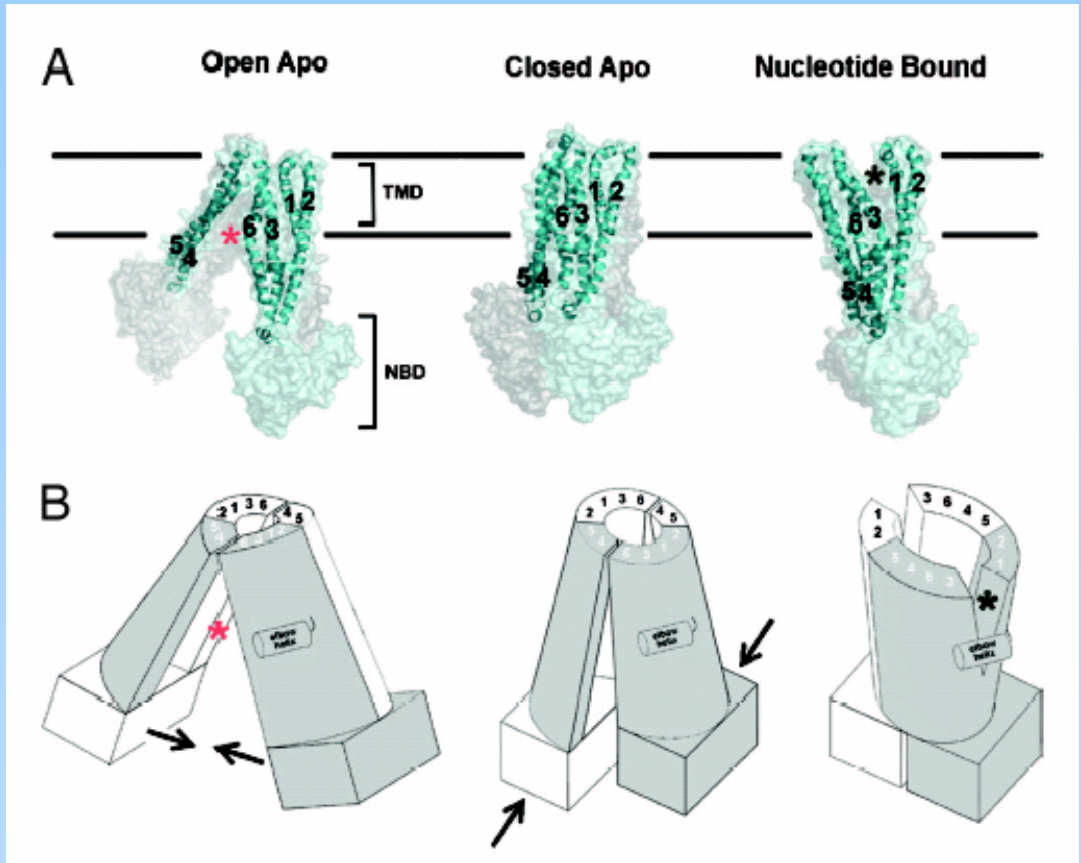

Reprocessed MsbA structures are consistent with distances from pulsed ESR and accessibility study by CW-ESR. Nucleotide-bound state of MsbA and SAV1688 are both consistent with pulse ESR.

What is ESR microscopy (ESRM)?

- ESR Microscopy (ESRM) is an imaging method aimed at obtaining spatially resolved spectroscopic magnetic resonance information from small samples with micron-scale resolution.

- The ESR signal originates from paramagnetic molecules/centers in the sample that may occur naturally, or can be added to the sample (similar to dyes in optics or contrast agents in NMR).

Why ESR Microscopy ?

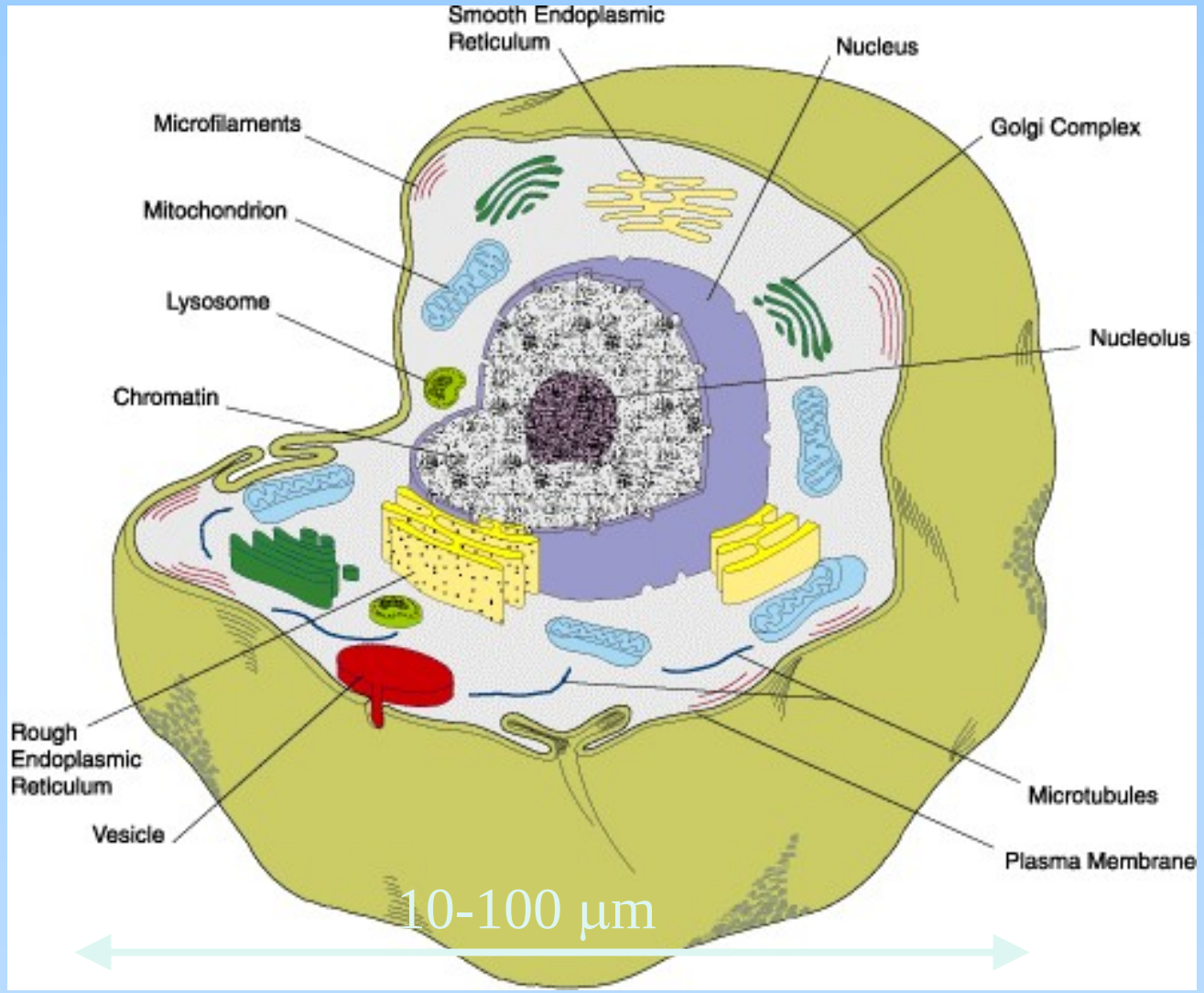

Taken from http://genetic-identity.com/Basic_Genetics/basic_genetics.html

ESRM vs. NMR microscopy

Significant efforts and funding have been invested in the past in the field of NMR microscopy. Recently even a combined NMR-optical microscope was demonstrated. What are the advantages of pursuing the similar, but less mature ESR imaging technology?

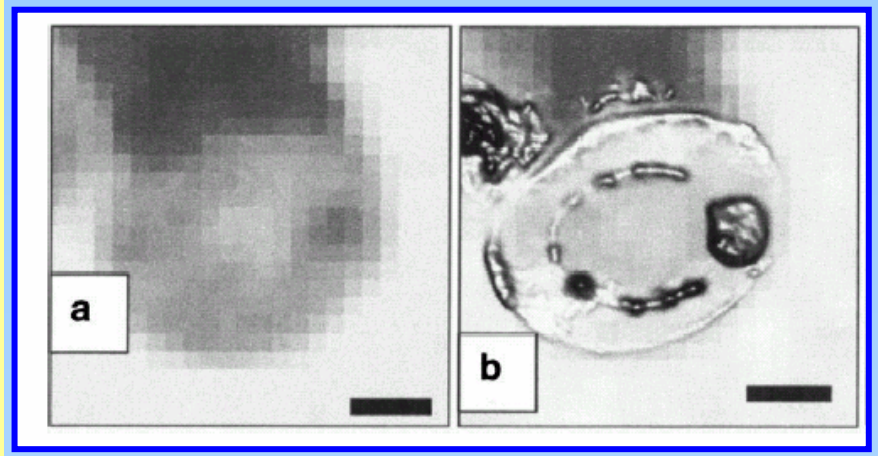

NMR, 20×20×100 μm Optical, 2×2×25 μm

- *ESR is more sensitive per spin.*
- *ESR resonators have higher Q than NMR micro-coils.*
- *ESR resolution is not limited by diffusion.*
- *ESR is More sensitive to dynamic effects.*

Goal: Resolution better than $[1mm]^3$ in several minutes.

- *Unique probes without "background" proton signal (radicals are added to the sample).*
- *Significantly less expensive magnet technology.*
- *Usually would require the addition of stable radicals (similar to fluorescent dyes or NMR contrast agents).*

The imaging probe

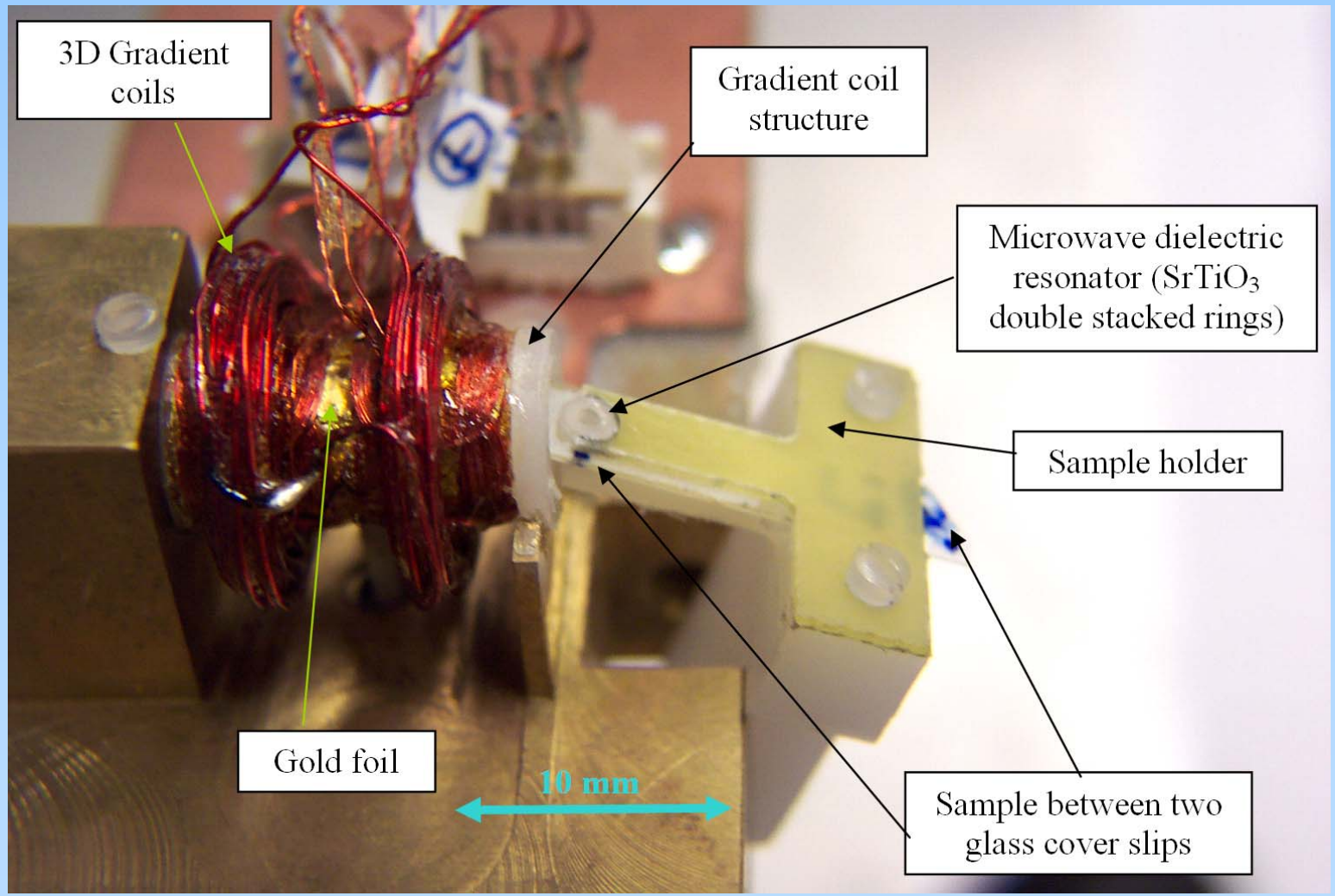

Pulse experimental results, 16 GHz

- 3 LiPc crystals.
- 25 min of acquisition time.
- Resolution of ~3×3×8 μm.
- Image size of 180×180×128 voxels.
- SNR ~550/voxel.

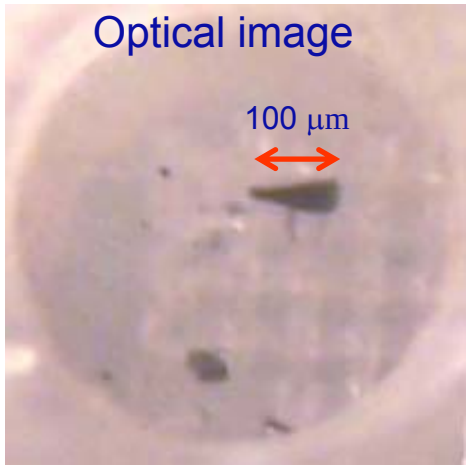

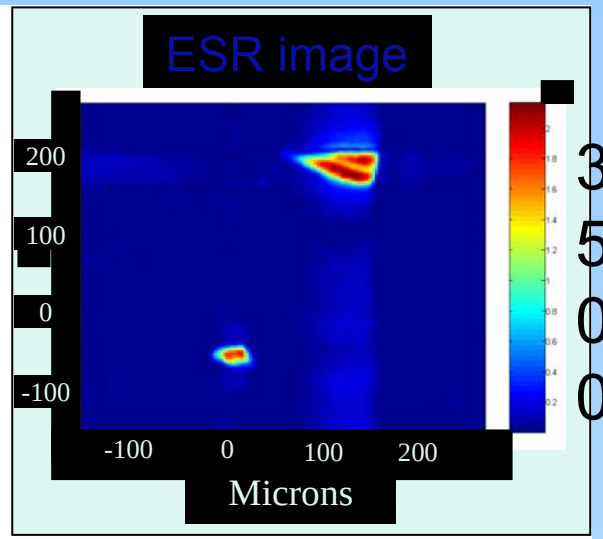

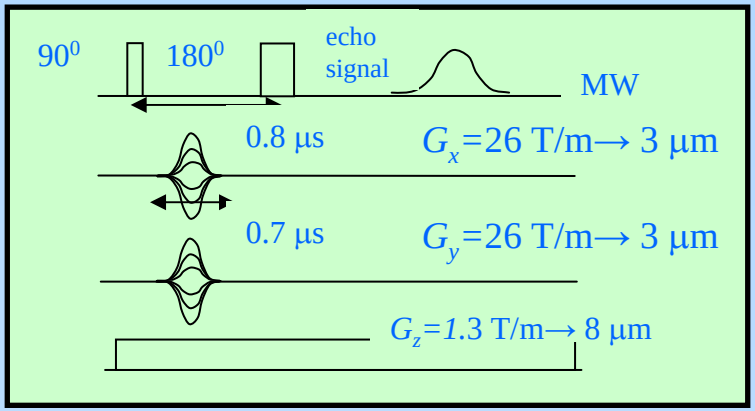

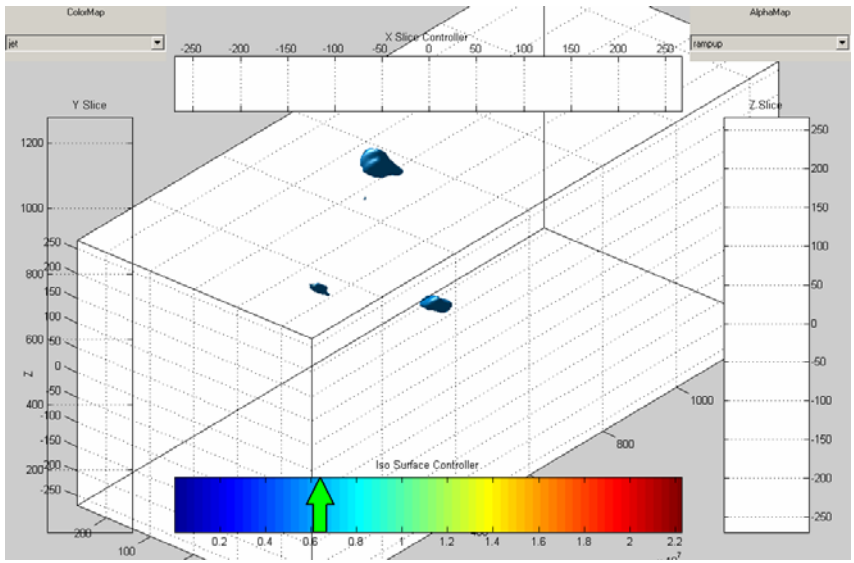

Initial Work on Applications, 16 GHz Pulsed Probe

- Drug release: in-vitro observation of slow release of trityl from polymer micro-spheres, and related phenomena.
- Here we observed the T_2 weighted image.

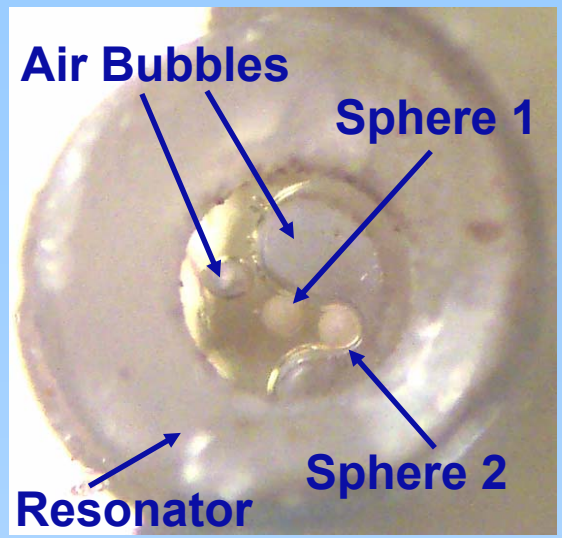

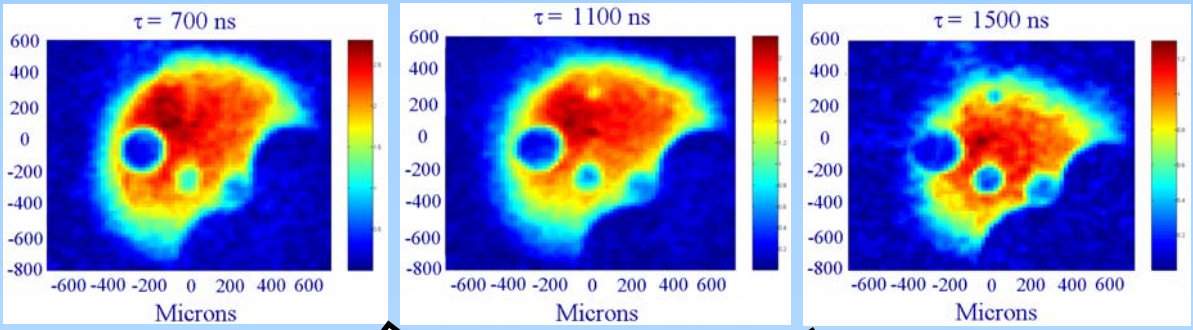

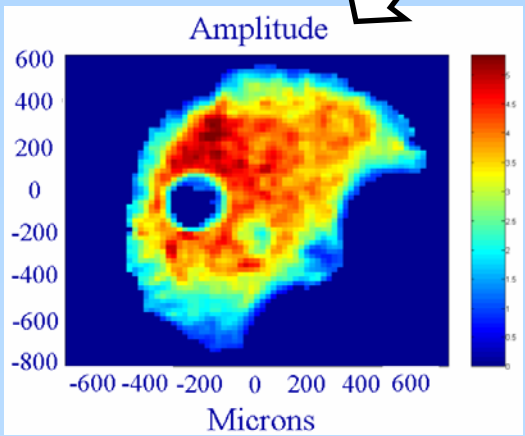

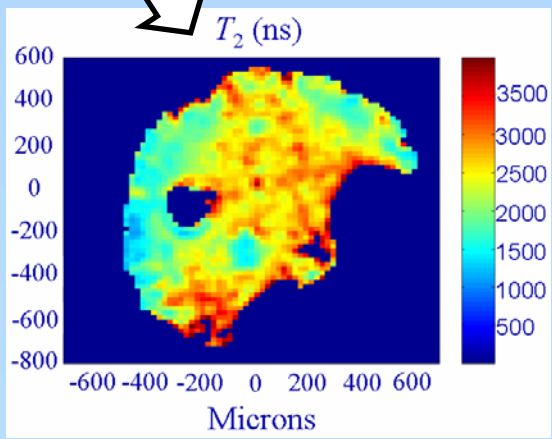

Shorter T_2, corresponds to "effective" viscosity of ~10 cP inside the sphere.

ACERT STAFF

Jaya Bhatnagar
Pëtr Borbat
Curt Dunnam
Boris Dzikovski
Keith Earle
Mingtao Ge
Elka Georgieva
Zhichun Liang
Jozef Moscicki
Andrew Smith
Dmitryi Tipikin
Joanne Trutko
Ziwei Zhang

Previous:
Aharon Blank
Yun-Wei Chiang
Wulf Höfbauer
Serguei Pachtchenko

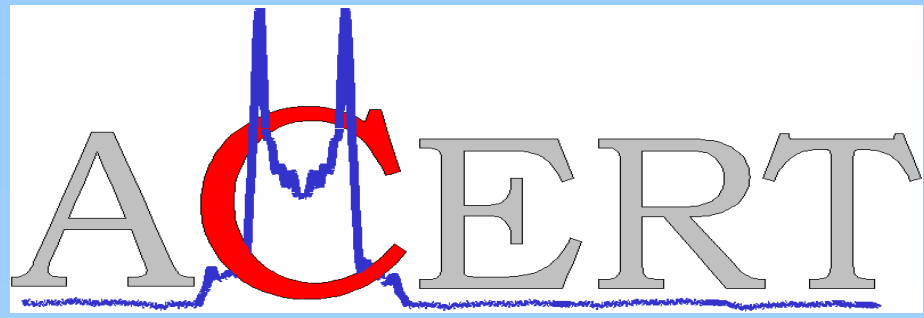

www.acert.cornell.edu

COLLABORATORS

Barbara Baird, Cornell Univ.
Brian Crane, Cornell Univ.
Wayne Hubbell, UCLA
Hassane Mchaourab, Vanderbilt Univ.
Benoit Roux, Univ. of Chicago
Deniz Sezer, Cornell Univ./Univ. of Chicago

The End